Eindhoven University of Technology

MASTER

Acoustics of slowly varying inlet ducts with arbitrary cross-section

Iyer, Akshay Ganesh

Award date:
2011

Link to publication

Acoustics of slowly varying inlet ducts with arbitrary cross-section

Author:
Akshay IYER

Supervisor:
S.W. RIENSTRA

July 12, 2011

Contents

List of Figures

Acknowledgement

Chapter 1

Introduction

The study of the sound propagation of ducts, aptly called as duct-acoustics, was classically used in studying the sound characteristic of pipe musical instruments which are hard walled, in which the mean flow is practically absent. Thus the available theory [1] was enough for modeling purposes. But in the middle of the 20th century with the arrival of the jet age, jet powered passenger airliners started doing intercontinental flights all over the world. The advent of the fuel efficient turbofan engines also brought in serious levels of noise pollution, which soon became a grave problem, especially to the residential areas nearby the airport. This resulted into serious research into noise reduction of these engines, particularly from the intake which emits high frequency sounds during take-off and landing.

With the Mach number M, of the medium being zero, the governing equation for acoustic pressure reduces to a Helmholtz equation,

$$(\nabla^2 + k_0^2)P = 0 \tag{1.1}$$

whose solution is of the form,

$$P = A \exp(-\mathrm{i}\boldsymbol{k}_0 \cdot \boldsymbol{x}) \tag{1.2}$$

and the time harmonic pressure has the expression,

$$p = A \exp\left(-\mathrm{i}(\boldsymbol{k}_0 \cdot \boldsymbol{x} - \omega t)\right) \tag{1.3}$$

In absence of a boundary the solution given by 1.3, is called a plane wave, whose angular frequency is ω, and the vector $\boldsymbol{k}_0$ is called the wave number vector. Thus the general solution of the problem 1.1 will be a superposition of plane waves, when there are no source term present.From linearity, the solution of any acoustic problem with time-independent boundary conditions and medium can be written as the sum of frequency components. If the geometry is simple enough, we can even write the solution as a sum over simpler solutions which we call modes. The issue whether a family of simple solutions is rich enough

5

to form a basis to represent a general solution is a question on its own. These modes are closely related to an associated eigenvalue problem. Thus for a ducted object, this tool comes in very handy for solving the problems of aero-acoustics. The further discussion about the modes is postponed to chapter-4, where we will give gain some insights about the same.

In case of a jet engine, the intake duct is subjected to medium not being stagnant, which increase the complexity of the acoustic problem.The straight ducts were having issues of aerodynamics, which lead to change in intake design, from a straight circular duct, to a slowly varying circular duct with lined walls, for attenuating the sound. The rapid expanse of the commercial airliner industry, meant more aircrafts at the airport. This in turn lead to the increase of sound levels during take-off and landing, which caused noise pollution in the areas neighboring the airport. This lead to the necessity of newer methods of modeling the noise from the jet-intake. Which lead to the rapid development in the field of Computational Aero-acoustics, where super computers were employed to solve the acoustically approximated constitutive equations of fluid flow.

During 1930s, when quantum mechanics was the prime area of physical research, many an equation fell into the category of singular perturbations, where the techniques of formal asymptotics known till then failed. This lead to development of different methods to solve equations in quantum mechanics approximately. Different, yet intertwined time scales, inseparable spatial scales were common in this field, and thus one can say that the entire singular perturbation theory came into light for solving equations of quantum mechanics, and astronomy. For tackling the irregularities arising from the spatial domains, especially in the Schrödinger's wave equation, three people viz. Wentzel, Kramer, and Brillouin in 1926 developed a method, which became famous as the WKB Ansatz. The irregularities in the temporal domain lead to the development of method of multiple scales. It was later realized that the WKB method is a special case of method of multiple scales. And slowly, perturbation methods opened up a new window into the study of applied mathematics field which lead to a blend of analytics and numerics.

With the main flow in the engine falling a prey to the regular perturbation analysis, using the quasi 1D-gasdynamics theme, all that remained was to take care of the acoustic disturbances arising out of the rotor stator interactions. As we saw before, the sound in straight ducts without any mean flow can be treated as a Fourier transformed eigenmode, taken along the length of the duct. This can be extended to cases where we do have mean flows under certain conditions. But these models were not suitable enough to model the situation of slowly varying ducts which is generally found in modern day airliners. To solve this particular issue, enter the maverick, the WKB method.

The assumption of 'slowly varying' duct along the length, implied that the cross-section changed along the length at a very slow rate, thus kicking in the dreaded ϵ parameter, which represents any small disturbances. This condition of 'slowly varying', gave a chance for the WKB Ansatz to approximate the same Fourier transformed eigenmodes, but now with some assumptions. This analysis also provided an insight, how an acoustic perturbation, which originates as an acoustic eigenmode at the fan end of the duct, changes itself according to the change in the cross-sectional geometry. Thus a comprehensive work was done in the field of slowly changing circular ducts, using the above WKB analysis by Rienstra in [5].

The aircraft companies exercised restraint with the engine inlet design, fearing for the safety of passengers. They did what ever they could using the models for a circular slowly changing duct, and got out many an innovation in acoustically lined ducts. Nevertheless, the military aircrafts, which don't have regulations were given a free hand in designing the engine intakes. If one observes, no combat aircraft has a circular intake, and in fact, the same holds true for the many bombers and transport aircrafts. One among the long list of Soviet bombers, was the Myasishchev M-4(Molot), having elliptic intakes, rather than the conventional circular ones and it didn't have any noise regulation.

Figure 1.1: Non-circular duct profile of the CFM56 engine in a Boeing 737-500: Hamster Pouch

The Boeing company came out with 737-300 series in 1984, as the part of the second generation 737 series. As off the 300 series, the 737 is powered by the regular CFM-56, high-bypass turbofan aircraft engines made by CFM International (CFMI), but with a difference. The ducts are integrated with the wings in order to give a larger ground clearance, which resulted in having the shape of a Hamster pouch, as shown in figure-1.1.

This was a clear deviation from the regular 'slowly varying' circular cross-section design of the jet engines. Peake and Cooper-[6] on similar lines of that Rienstra-[5] did research on the 'slowly varying' elliptic hard walled ducts, which gave a new direction to this field. Rienstra-[3] generalized the theory for any arbitrary duct, but the with the acoustic lining coming into play, it became hard for solving the governing equations analytically. This called for numerical study of the governing equations, which happens to be the main theme of this master thesis.

Chapter 2

Equation of fluid Motion

2.1 Constitutive Law and constitutive equations

The laws of mass, momentum, and energy conservation, written in terms of pressure p, density ρ, particle velocity $\boldsymbol{v}$, viscous stress tensor $\boldsymbol{\tau}$, internal energy e, and heat flux $\mathbf{q}$, are given by;

$$mass: \quad \frac{\partial}{\partial t}\rho + \nabla \cdot (\rho \boldsymbol{v}) = 0 \tag{2.1a}$$

$$momentum: \quad \frac{\partial}{\partial t}(\rho \boldsymbol{v}) + \nabla \cdot (\rho \boldsymbol{v}\boldsymbol{v}) = -\nabla p + \nabla \cdot \boldsymbol{\tau} \tag{2.1b}$$

$$energy: \quad \frac{\partial}{\partial t}(\rho E) + \nabla \cdot (\rho E \boldsymbol{v}) = -\nabla \cdot \mathbf{q} - \nabla \cdot (p\boldsymbol{v}) + \nabla \cdot (\boldsymbol{\tau}\boldsymbol{v}) \tag{2.1c}$$

where

$$E = e + \frac{1}{2}v^2$$

The enthalpy i, is given by;

$$i = e + \frac{p}{\rho} \tag{2.2}$$

The first law of thermodynamics says that, $\mathrm{d}Q = \mathrm{d}e + p\mathrm{d}(1/\rho)$, where $\mathrm{d}Q$, is the external heat added to the system, and $p\mathrm{d}(1/\rho)$, is the work done by the reversible process. Also, for a reversible process, Clausius equality says that, $\mathrm{d}Q = T\mathrm{d}s$ for entropy s. Therefore, one can get the following relation, in combination with equation, 2.2.

$$T\mathrm{d}s = \mathrm{d}e + p\mathrm{d}\left(\frac{1}{\rho}\right) = \mathrm{d}i - \frac{\mathrm{d}p}{\rho} \tag{2.3}$$

With $\frac{\mathrm{d}}{\mathrm{d}t} = \frac{\partial}{\partial t} + \mathbf{v} \cdot \nabla$ for the convective derivative, the above conservation laws may be reduced to

$$mass: \qquad \frac{\mathrm{d}}{\mathrm{d}t}\rho = -\rho\nabla\cdot\boldsymbol{v} \tag{2.4a}$$

$$momentum: \quad \rho\frac{\mathrm{d}}{\mathrm{d}t}\boldsymbol{v} = -\nabla p + \nabla\cdot\boldsymbol{\tau} \tag{2.4b}$$

$$energy: \quad \rho T\frac{\mathrm{d}}{\mathrm{d}t}s = -\nabla\cdot\mathbf{q} + \boldsymbol{\tau}{:}\nabla\boldsymbol{v} \tag{2.4c}$$

2.2 Inviscid and isentropic acoustic regime

The journey into acoustics begins, with non-dimensionalizing the equations, 2.4a, 2.4b, 2.4c, with a suitable scaling;

$$\mathbf{x} := L\mathbf{x}, \quad \boldsymbol{v} := v_{\mathrm{ref}}\,\boldsymbol{v}, \quad t := \frac{L}{v_{\mathrm{ref}}}t, \quad \rho := \rho_{\mathrm{ref}}\,\rho$$

$$\mathrm{d}p := \rho_{\mathrm{ref}}\,v_{\mathrm{ref}}^2\,\mathrm{d}p, \quad \boldsymbol{\tau} := \frac{\mu v_{\mathrm{ref}}}{L}\tau, \quad \mathbf{q} := \frac{\kappa\Delta T}{L}\mathbf{q}$$

$$T := T_0 T, \quad \mathrm{d}T := \Delta T\mathrm{d}T, \quad \mathrm{d}s := \frac{C_p\Delta T}{T_{\mathrm{ref}}}\mathrm{d}s$$

to get;

$$\frac{\mathrm{d}}{\mathrm{d}t}\rho = -\rho\nabla\cdot\boldsymbol{v} \tag{2.5}$$

$$\rho\frac{\mathrm{d}}{\mathrm{d}t}\boldsymbol{v} = -\nabla p + \frac{1}{Re}\nabla\cdot\boldsymbol{\tau} \tag{2.6}$$

$$\rho T\frac{\mathrm{d}}{\mathrm{d}t}s = -\frac{1}{Pe}\nabla\cdot\mathbf{q} + \frac{Ec}{Re}\boldsymbol{\tau}:\nabla\boldsymbol{v} \tag{2.7}$$

In the acoustic regime, it is assumed that, the viscous, and turbulent stress terms play a negligible role in the acoustic refime, and the acoustic perturbations are too fast to be affected by the thermal conduction. This results in considering infinite Reynolds number Re, and infinite Peclet Number Pe. We also assume a perfect gas and thus we have constant heat capacities C_V, and C_P.

$$\frac{\mathrm{d}}{\mathrm{d}t}\rho = -\rho\nabla\cdot\boldsymbol{v} \tag{2.8}$$

$$\rho\frac{\mathrm{d}}{\mathrm{d}t}\boldsymbol{v} = -\nabla p \tag{2.9}$$

$$\frac{\mathrm{d}}{\mathrm{d}t}s = 0 \tag{2.10}$$

10

This implies that the entropy remains constant along the streamlines. Furthermore, we assume gas to be perfect, and we have the following relations;

$$\mathrm{d}s = C_V \frac{\mathrm{d}p}{p} - C_P \frac{\mathrm{d}\rho}{\rho}, \tag{2.11}$$

$$c^2 = \gamma p/\rho \tag{2.12}$$

$$\frac{\mathrm{d}}{\mathrm{d}t}p = c^2 \frac{\mathrm{d}}{\mathrm{d}t}\rho \tag{2.13}$$

Where, C_V, and C_P are specific heat capacities at constant volume, and constant pressure respectively, and $\gamma = \frac{C_P}{C_V}$ is the adiabatic gas constant.

2.3 The acoustically perturbed flow

It is assumed, that the mean flow is homentropic(s is uniformly constant). Consider, a stationary mean flow with unsteady perturbations, given by;

$$\boldsymbol{v} = \boldsymbol{v}_0 + \boldsymbol{v}' \quad , p = p_0 + p', \quad \rho = \rho_0 + \rho', \quad s = s_0 + s' \tag{2.14}$$

Substituting the above perturbations in equations, 2.8, 2.9, and 2.10, and linearizing for small amplitude, one gets the equation for the mean flow, as;

$$\nabla \cdot (\rho_0 \boldsymbol{v}_0) = 0 \tag{2.15a}$$

$$\rho_0 (\boldsymbol{v}_0 \cdot \nabla) \boldsymbol{v}_0 = -\nabla p_0 \tag{2.15b}$$

$$(\boldsymbol{v}_0 \cdot \nabla) s_0 = 0 \tag{2.15c}$$

while

$$ds_0 = C_V \frac{dp_0}{p_0} - C_P \frac{d\rho_0}{\rho_0} \quad c_0^2 = \frac{\gamma p_0}{\rho_0} \tag{2.16}$$

The equations governing the perturbations are given by;

$$\frac{\partial \rho'}{\partial t} + \nabla \cdot (\boldsymbol{v}_0 \rho' + \boldsymbol{v}' \rho_0) = 0 \tag{2.17a}$$

$$\rho_0 (\frac{\partial}{\partial t} + \boldsymbol{v}_0 \cdot \nabla) \boldsymbol{v}' + \rho_0 (\boldsymbol{v}' \cdot \nabla) \boldsymbol{v}_0 + \rho' (\boldsymbol{v}_0 \cdot \nabla) \boldsymbol{v}_0 = -\nabla p' \tag{2.17b}$$

$$(\frac{\partial}{\partial t} + \boldsymbol{v}_0 \cdot \nabla) s' + \boldsymbol{v}' \cdot \nabla s_0 = 0 \tag{2.17c}$$

while assuming that $s'_{init} = 0$,

$$s' = \frac{C_V}{p_0} p' - \frac{C_V}{\rho'} \rho_0 = \frac{C_V}{p_0} (p' - c_0^2 \rho') \tag{2.18}$$

11

From equation, 2.13, one can get for the mean flow that $\mathbf{v}_0 \cdot \nabla p_0 = c_0^2 \mathbf{v}_0 \cdot \nabla \rho_0$. Since the mean flow is homentropic ($s_0 = const$), $\Rightarrow \quad \nabla p_0 = c_0^2 \nabla \rho_0$, while the perturbations are isentropic along the streamlines. When the entire flow is homentropic, the pressure and density perturbation are related by the usual;

$$p' = c_0^2 \rho' \tag{2.19}$$

The linearity of sound waves allows us to build up an acoustic field as a sum of simpler solutions of wave equation. Therefore, one can think of the acoustic waves as time harmonic or as a Fourier transform into the frequency domain. Hence one can write;

$$\boldsymbol{v}' = \text{Re}(\hat{\boldsymbol{v}} e^{i\omega t}), \quad p' = \text{Re}(\hat{p} e^{i\omega t}), \quad \rho' = \text{Re}(\hat{\rho} e^{i\omega t}), \quad s' = \text{Re}(\hat{s} e^{i\omega t}) \tag{2.20}$$

the equations 2.17a,2.17b, 2.17c, and 2.18 can be written in complex form as;

$$i\omega\hat{\rho} + \nabla \cdot (\boldsymbol{v}_0\hat{\rho} + \hat{\boldsymbol{v}}\rho_0) = 0 \tag{2.21}$$

$$\rho_0(i\omega + \boldsymbol{v}_0 \cdot \nabla)\hat{\boldsymbol{v}} + \rho_0(\hat{\boldsymbol{v}} \cdot \nabla)\boldsymbol{v}_0 + \hat{\rho}(\boldsymbol{v}_0 \cdot \nabla)\boldsymbol{v}_0 = -\nabla\hat{p} \tag{2.22}$$

$$(i\omega + \boldsymbol{v}_0 \cdot \nabla)\hat{s} + \hat{\boldsymbol{v}} \cdot \nabla s_0 = 0 \tag{2.23}$$

$$\hat{s} = \frac{C_v}{p_0}(\hat{p} - c_0^2\hat{\rho}) \tag{2.24}$$

2.3.1   Irrotational isentropic flow

When the flow is irrotational and isentropic everywhere, then one can introduce a potential for the velocity, where $\mathbf{v} = \nabla\phi$, and can express ρ, a function of p only. These relations, makes the provision for integrating the momentum equation, and getting the following simplification;

$$\frac{\partial}{\partial t}\phi + \frac{1}{2}v^2 + \frac{c^2}{\gamma - 1} = \text{const}, \quad \frac{p}{\rho^\gamma} = \text{const} \tag{2.25}$$

Taking a cue from the above equation, one can apply to the same to the mean flow with time harmonic perturbation, with the velocity potential given by; $\phi = \phi_0 + \text{Re}(\hat{\phi} e^{i\omega t})$. Thus, with the information that $\frac{\partial}{\partial t}\phi_0 = 0$, one can rewrite the equation 2.25, for the mean flow as;

$$\frac{1}{2}v_0^2 + \frac{c_0^2}{\gamma - 1} = \text{const} \tag{2.26}$$

$$\nabla \cdot (\rho_0 \boldsymbol{v}_0) = 0 \tag{2.27}$$

$$\frac{p_0}{\rho_0^\gamma} = \text{const} \tag{2.28}$$

and for the acoustic perturbation as;

$$(i\omega\boldsymbol{v}_0 \cdot \nabla)\hat{\rho} + \hat{\rho} + \hat{\rho}\nabla \cdot \boldsymbol{v}_0 + \nabla \cdot (\rho_0\nabla\hat{\phi}) = 0 \tag{2.29}$$

$$\rho_0(i\omega + \boldsymbol{v}_0 \cdot \nabla)\hat{\phi} + \nabla\hat{p} = 0 \tag{2.30}$$

$$\hat{p} = c_0^2\hat{\rho} \tag{2.31}$$

12

Eliminating the $\hat{\rho}$, and $\hat{p}$, from the above equations, and using equation 2.15a, a generalized convected wave equation is obtained;

$$\frac{1}{\rho_0}\nabla \cdot (\rho_0 \nabla \hat{\phi}) - (\mathrm{i}\omega + \boldsymbol{v}_0 \cdot \nabla)\left[\frac{1}{\mathrm{c}_0^2}(\mathrm{i}\omega + \boldsymbol{v}_0 \cdot \nabla)\hat{\phi}\right] = 0 \tag{2.32}$$

2.4   The boundary condition

We have a lined a duct which is impenetrable for steady mean flow. Myers-[8] has given a detailed description of for curved boundary walls, which for us becomes very important. Here we give a brief description of the boundary condition as obtained by Myers. The research carried out by Ingard-[9], and followed by its review by Nayfeh, Kaiser and Telionis-[18], lead to the conclusion that, when the mean flow is treated as inviscid the proper kinematic condition at an impenetrable boundary of the acoustic field is expressed physically by the requirement of continuity of acoustic particle displacement. This means specifically that at any such surface which generates an acoustic field by small deformations, or undergoes small deformations in response to an acoustic field, the acoustic fluid particle displacement in the direction normal to the undeformed boundary must equal the displacement of the boundary itself in the same direction.

Consider a control surface S along the duct wall S_0, described by the relation

$$f(\boldsymbol{x}, t) = 0 \tag{2.33}$$

then, provided that f is defined so that it is positive on the fluid side of S and negative on the other, the normal vector, $\boldsymbol{n}(t)$ is given by

$$\boldsymbol{n}(t) = \nabla f/|\nabla f| \tag{2.34}$$

When we differentiate 2.33, with respect to t, using the material derivative, to obtain

$$\nabla f \cdot \frac{\mathrm{d}}{\mathrm{d}t}\boldsymbol{x} = -\frac{\partial f}{\partial t} \text{ on } f = 0 \tag{2.35}$$

The above equation can be further simplified to be the written as

$$\boldsymbol{v} \cdot \nabla f = -\frac{\partial f}{\partial t} \text{ on } f = 0 \tag{2.36}$$

For our case, control surface S corresponds to the interface between the mean flow in the duct and a (postulated) very thin layer next to the duct wall S_0 with zero mean flow. Now to describe the situation, we introduce local curvilinear, orthogonal coordinate system, $a(\boldsymbol{x})$, $b(\boldsymbol{x})$, $c(\boldsymbol{x})$, fixed on S_0, such that $a(\boldsymbol{x}) = 0$ on S_0. That is , the coordinate $a(\boldsymbol{x})$, is chosen in such a manner that it is normal to S_0, and the other two lie tangentially on S_0. Then the

surface $S(t)$, can be described as $a = \epsilon g(b, c, t) + \mathcal{O}(\epsilon^2)$. Now here ϵ, characterizes the magnitude of acoustic perturbation, which we had dealt in a direct manner in the previous section.

The relation 2.33, can be now written as $a - \epsilon g(b, c, t) + \mathcal{O}(\epsilon^2) = 0$, and as we saw in the previous section, the velocity $\boldsymbol{v}$, can be written as $\boldsymbol{v} = \boldsymbol{v}_0 + \boldsymbol{v}'$, where $\boldsymbol{v}' = \epsilon\tilde{\boldsymbol{v}}$. Now 2.36 becomes

$$(\boldsymbol{v}_0 + \epsilon\tilde{\boldsymbol{v}} + ...) \cdot \nabla(a - \epsilon g + ...) - \epsilon\frac{\partial}{\partial t}(g + ...) = 0 \text{ on } a = \epsilon g + ... \tag{2.37}$$

Now using the methods of formal asymptotics and linearizing the boundary condition, one can get the boundary condition for the acoustic perturbation on the stationary mean surface S_0 as,

$$\tilde{\boldsymbol{v}} \cdot \boldsymbol{n} = (\frac{\partial}{\partial t} + \boldsymbol{v}_0 \cdot \nabla)(g/|\nabla a|) - (g/|\nabla a|)\boldsymbol{n} \cdot (\boldsymbol{n} \cdot \nabla\boldsymbol{v}_0) \text{ on } S_0 \tag{2.38}$$

Condition 2.38 is expressed without specific reference to the local orthogonal curvilinear coordinate system. Its easy for us using condition 2.38 to get a boundary condition appropriate to an acoustically absorbing boundary whose normal impedance Z for harmonic motion is known. The pressure across the interface S is continuous, while the velocity has a jump given by relation 2.37 or 2.38. Assuming the boundary condition $p = Z(\boldsymbol{v} \cdot \boldsymbol{n})$ along the wall and thus on the wall side of S, we can translate this into a condition on the flow side of S.

$$i\omega(\tilde{\boldsymbol{v}} \cdot \boldsymbol{n}) = [i\omega + \boldsymbol{v}_0 \cdot \nabla - \boldsymbol{n} \cdot (\boldsymbol{n} \cdot \nabla\boldsymbol{v}_0)]\left(\frac{\tilde{p}}{Z}\right) \tag{2.39}$$

With the acoustic perturbation, and the main fluid flow separated, we can now go to carry on further analysis of these equations using the asymptotic methods held at our disposal.

14

Chapter 3

Mean flow: Quasi 1D Gasdynamics

In this chapter, we deal mainly with the equations that govern the mean flow inside the duct. Its will be very interesting in the further chapters, that the mean flow is a case of regular perturbation. Thus a simple asymptotic analysis, a posteriori to a proper scaling can reduce the complexity of the problem drastically.

3.1 Method of slow variation

We have a slowly varying duct, in one direction, say x, with arbitrary cross section. The mean flow in this duct is given by the equations, 2.26, 2.27, and 2.28. Since we have assumed an, irrotational, homentropic flow, taking cue from the section 2.3.1, we can write, $\boldsymbol{v}_0 = \nabla \phi_0$. Let the variations in the horizontal direction, x, be of, $\mathcal{O}(\epsilon^{-1})$. Thus in order to find the changes in variables, and parameters, due to this varying geometry in one direction, one must slow down the variation in x, and look into the same. Therefore, a new slow variable is introduced to observe the change, in the following manner, $X = \epsilon x$. This new variable X, is of order $\mathcal{O}(1)$, thus varies slowly compared to its faster kin, x. Let the duct surface S be given by the function $\tilde{f}(x, r, \theta; \epsilon) = 0$, with the normal oriented positive on the surface facing the flow. Slow variation implies that one can write $\tilde{f}(x, r, \theta; \epsilon) = f(X, r, \theta; \epsilon)$, and that this function is assumed to have a uniform asymptotic expansion of the form $f(\epsilon x, r, \theta; \epsilon) = f_0(X, r, \theta) + \epsilon f_1(X, r, \theta) + \mathcal{O}(\epsilon^2)$. In this section, when we refer to the surface S, it will always be in reference to $\mathcal{O}(1)$ term, $f(X, r, \theta) = f_0(X, r, \theta)$. The mean mass flux flow across any given cross-sectional area is a constant and is given by the following equation

$$\iint_A \rho_0 \phi_{0,x} dS = \iint_A \rho_0 \epsilon \phi_{0,X} = \mathcal{F} \tag{3.1}$$

The flux $\mathcal{F}$, is considered of $\mathcal{O}(1)$, thus, this forms a lead to have the velocity potential scaled and to be given by, $\phi_0 = \frac{1}{\epsilon} \Phi(X, r, , \theta)$. Similarly, the density, pressure, and the speed of sound will be, $\rho_0 = \rho_0(X, r, \theta)$, and $p_0 = p_0(X, r, \theta)$, and $c_0 = c_0(X, r, \theta)$, respectively.

15

For convenience, one can write the gradient operator as;

$$\nabla = \frac{\partial}{\partial x}\boldsymbol{e}_x + \nabla_\perp \tag{3.2}$$

As the variation is in only one direction, which implies that the orthogonal coordinates are free from ϵ. Therefore one can rewrite the divergence, and the gradient as follows;

$$\nabla \cdot = \epsilon \frac{\partial}{\partial X}() + \nabla_\perp \cdot () \tag{3.3}$$

$$\nabla = \epsilon \frac{\partial}{\partial X}()\boldsymbol{e}_X + \nabla_\perp() \tag{3.4}$$

Moreover, the impermeability of the wall gives, $\nabla\Phi \cdot \nabla f = 0$, and the mass flux happens to be constant, at any given cross section of the duct(which depends on X), which implies

$$\iint_{A(X)} \rho_0 \Phi_x \mathrm{dS} = \mathcal{F}, \quad \forall \mathrm{X} \tag{3.5}$$

Using the equations, 3.3, and 3.5, along with $\boldsymbol{v}_0 = \frac{1}{\epsilon}\nabla\Phi(X, r, \theta)$, in equations, 2.26, 2.27, one gets;

$$\epsilon^2 \frac{\partial}{\partial X}\left(\rho_0 \frac{\partial}{\partial X}\Phi\right) + \nabla_\perp \cdot (\rho_0 \nabla_\perp \Phi) = 0 \tag{3.6}$$

$$\frac{1}{2}\left(\Phi_X^2 + \epsilon^{-2}|\nabla_\perp\Phi|^2\right) + \frac{\rho_0^{\gamma-1}}{\gamma-1} = \mathcal{E} \tag{3.7}$$

Equation 3.7, is obtained by also combining the fact, that $c_0^2 = \frac{\gamma p_0}{\rho_0}$, and equation 2.28. The impermeability condition gives;

$$\nabla\Phi \cdot \nabla f = \epsilon^2 \Phi_X f_X + \nabla_\perp\Phi \cdot \nabla_\perp f = 0, \quad at\ f = 0 \tag{3.8}$$

We can see that, all the equation depends on ϵ^2, thus it natural to take our asymptotic expansions for the parameters, to the powers of ϵ^2, as follows;

$$\Phi = \Phi_0(X, r, \theta) + \mathcal{O}(\epsilon^2), \quad \rho_0 = D_0(X, r, \theta) + \mathcal{O}(\epsilon^2), \quad p_0 = P_0(X, r, \theta) + \mathcal{O}(\epsilon^2) \tag{3.9}$$

Substituting, for Φ, from equation 3.9, in the Bernoulli's equation, 3.7, and matching the orders of LHS, and RHS, one can get that, $|\nabla_\perp\Phi_0|^2 = 0$. Thus, $\Phi_0 = \Phi_0(X)$, and using the same Bernoulli's equation, it can be seen from the $\mathcal{O}(1)$ terms, that $D_0 = D_0(X)$. The RHS, of 3.5 is of $\mathcal{O}(1)$, and substituting for ρ_0, and Φ, from 3.9, the following result is obtained;

$$\iint_{A(X)} D_0(X)\Phi_0(X)_X = \mathcal{F} \quad \Rightarrow \quad \Phi_0(X)_X = U_0(X) = \frac{\mathcal{F}}{D_0(X)A(X)} \tag{3.10}$$

16

The mean flow velocity, $\boldsymbol{v}_0$, can be represented as, $\boldsymbol{v}_0 = U\boldsymbol{e}_x + \boldsymbol{V}_\perp$. We also know that, $\boldsymbol{v}_0 = \nabla\phi_0 = \frac{1}{\epsilon}\nabla\Phi$, hence we can write using 3.4 that;

$$U\boldsymbol{e}_x + \boldsymbol{V}_\perp = \Phi_X\boldsymbol{e}_x + \frac{1}{\epsilon}\nabla_\perp\Phi \tag{3.11}$$

Since $\Phi = \mathcal{O}(1)$, the above equation yields that, $U = \mathcal{O}(1)$, and $\boldsymbol{V}_\perp = \mathcal{O}(\epsilon)$. Combining equation 3.9, and the fact that $\Phi_0 = \Phi_0(X)$ we can get that;

$$U = U_0(X) + \mathcal{O}(\epsilon^2), \quad \boldsymbol{V}_\perp = \epsilon\boldsymbol{V}_{\perp 0} + \mathcal{O}(\epsilon^3) \tag{3.12}$$

The asymptotic expansions as given by 3.9 can be substituted into the Bernoulli's equation 3.7, to get;

$$\frac{1}{2}\left(\left[\Phi_0(X) + \mathcal{O}(\epsilon^2)\right]_X\right)^2 + \epsilon^{-2}\left[\nabla_\perp(\Phi_0 + \mathcal{O}(\epsilon^2))\right]^2 + \frac{(D_0(X) + \mathcal{O}(\epsilon^2))^{\gamma-1}}{\gamma - 1} = \mathcal{E} \tag{3.13}$$

Approximating the above equation to the leading order and using the facts that $\nabla_\perp\Phi_0 = 0$, and $U_0(X) = \Phi_0(X)_X$, we get 3.13. With the substitution of expression of $U_0(X)$, from 3.10, in 3.13, the Bernoulli's equation is transformed into the following algebraic equation in one variable with $D_0(X)$, as the unknown, given by;

$$\frac{\mathcal{F}^2}{2D_0^2 A^2} + \frac{D_0^{\gamma-1}}{\gamma - 1} = \mathcal{E} \tag{3.14}$$

where, γ is the adiabatic gas coefficient.

3.2 The Mean Flow Parameters

All the parameters are dimensionless in nature, we need to find expressions for dimensionless area A, and dimensionless flux $\mathcal{F}$, so as to calculate the mean flow density using equation-3.14. Consider $\mathcal{F}'$, as the dimensional mass flux. Let the area of the cross-section at beginning of the intake duct be given A_{ref}, then the reference radius R_{ref}, is given by:

$$R_{\text{ref}} = \sqrt{\frac{A_{\text{ref}}}{\pi}}$$

Therefore, at each cross-section the area is made dimensionless using the above reference radius, as follows:

$$A(X) = \frac{A'(X)}{R_{\text{ref}}^2} \tag{3.15}$$

Where $A'(X)$, is the dimensional area of the cross-section at the given point X. In the problem, all the reference values such as, ρ_{ref}, and v_{ref}, etc, are taken to be the values of

17

the same obtained at the beginning of the intake duct. The speed of sound can also be made dimensionless by taking the reference as the beginning of the duct, and can be re-written as, $C = C_{\text{ref}} \; C_0$. Now, armed with these things, one can go on to obtain an expression for the dimensionless mass flux $\mathcal{F}$. We know that the flux remains constant through all the cross section, owing to the approximation of slowly varying duct, thus:

$$\mathcal{F}' = \iint_A \rho v \, ds = A_{\text{ref}} \; \rho_{\text{ref}} \; v_{\text{ref}} \tag{3.16}$$

Which further can be manipulated in writing:

$$\mathcal{F}' = \frac{A_{\text{ref}} \; \rho_{\text{ref}} \; v_{\text{ref}}}{R^2_{\text{ref}} \; \rho_{\text{ref}} \; C_{\text{ref}}} R^2_{\text{ref}} \; C_{\text{ref}} \; \rho_{\text{ref}} \; = \mathcal{F} \rho_{\text{ref}} \; C_{\text{ref}} \; R^2_{\text{ref}} \tag{3.17}$$

Thus the dimensionless mass flux can be written as;

$$\mathcal{F} = \frac{A_{\text{ref}} \; \rho_{\text{ref}} \; v_{\text{ref}}}{R^2_{\text{ref}} \; \rho_{\text{ref}} \; C_{\text{ref}}} = \pi M_{\text{ref}} \tag{3.18}$$

Where M_{ref} happens to be the Mach number at the beginning of the duct. With knowledge of the value of $\mathcal{F}$, one can proceed to find the value of the integration constant in equation-3.14. The constant, $\mathcal{E}$, is again obtained at the beginning of the duct, where dimensionless density $D_0 = 1$, and dimensionless area $A = \pi$. Substituting these values in 3.14, we get an expression for the integration constant.

$$\mathcal{E} = \frac{M^2_{\text{ref}}}{2} + \frac{1}{\gamma - 1} \tag{3.19}$$

The attention now turns to find a suitable expression for the dimensionless speed of sound $C_0(X)$, in terms of mean flow density $D_0(X)$. The assumption of having an isentropic mean flow, gives us the lead in finding the expression with the relation of speed of sound

$$C^2 = \frac{\gamma P}{\rho} \tag{3.20}$$

Thus at the reference point we have:

$$P_{\text{ref}} \; = \frac{C^2_{\text{ref}} \; \rho_{\text{ref}}}{\gamma} \tag{3.21}$$

This information, along with the other scaled parameters transform 3.20

$$C_0^2 = \frac{P}{D_0} \tag{3.22}$$

where the P is dimensionless. Now the assumption of homentropy gives another important relation, given by:
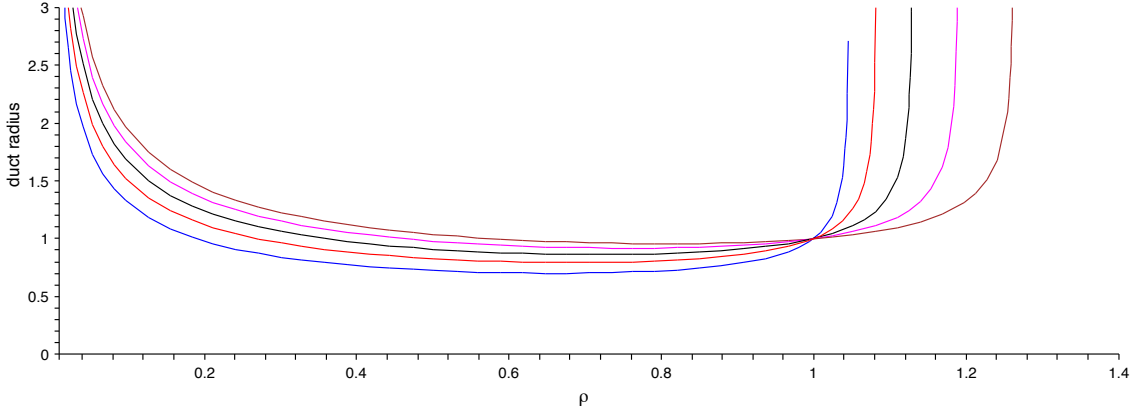
$$\frac{P}{\rho^\gamma} = const \tag{3.23}$$

18

Figure 3.1: Density vs Duct radius for Mach numbers M=0.3 to 0.7(in steps of 0.1)

Thus with mathematical manipulation one can find the relation for dimensionless pressure of mean flow.

$$P = D_0^\gamma \tag{3.24}$$

Hence, from 3.22 and 3.24, we have a expression for the dimensionless speed of sound at each and every cross section.

$$C_0(X) = D_0(X)^{(\gamma-1)/2} \tag{3.25}$$

With the expressions obtained for constants, the mean flow equation-3.14 becomes a non-linear algebraic equation in $D_0(X)$, which has to be solved for every cross-section for the same. For finding the solution, we go back to Newton's method for finding out the density, D_0. But, the choice of the parameters governing the geometry ought to be taken with care, because the entire analysis is based on slowly varying duct. This puts extra restraints on the choice of of our cross-section. With the premise that the mass flux $\mathcal{F}$ is constant, implies that the density cannot vary too much from the reference point value. Thus, this leads to do some analysis regarding how much one can vary slowly.

Using, equation-3.14, one can write dimensionless area $A(X)$, as a function of density $D_0(X)$ as:

$$A^2 = \frac{(\gamma-1)\pi^2 M^2}{D_0^2\left(2 + (\gamma-1)M^2 - 2D_0^{\gamma-1}\right)} \tag{3.26}$$

From 3.26 one can obtain a measure for the dimensionless radius. One should note that, though we don't have a circular geometry all along, at each cross-section we can find a radial measure for the given cross section. With this in place, an estimate can be made of how much one can change the geometry to have the condition of 'slowly varying'. In figure-3.1 we get an insight of the density affects the duct radius and vice-versa. We see that, as the Mach number increases, the graph profile starts moving upwards, and to its
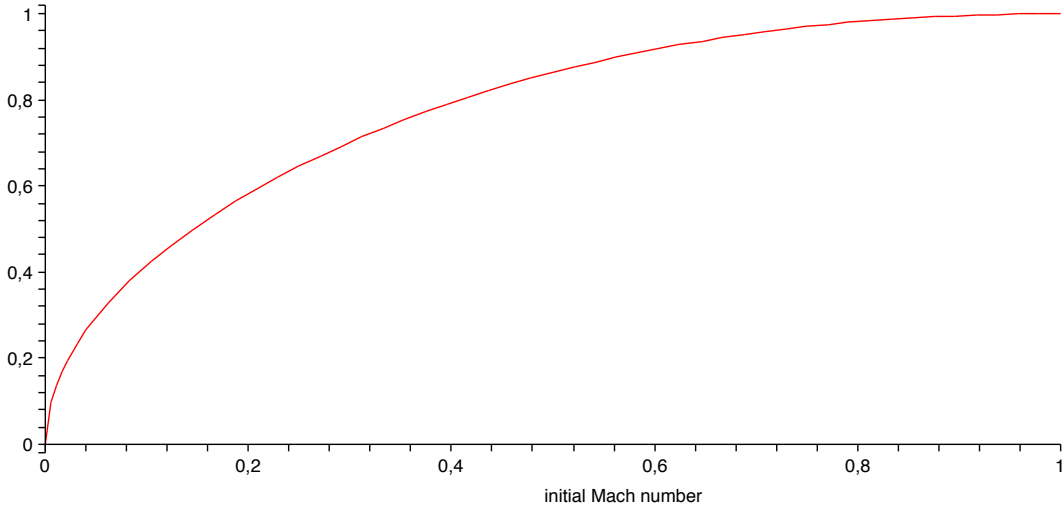
Figure 3.2: Mach Number vs Minimum Radius $R_{\min}$

right. Hence, the graph in all gives us a preliminary idea about the choice of our radial parameters for getting appropriate realistic values.

All our calculation associated with the mean flow along the duct is associated with referential values at the opening of the duct. We now find out the expression for density associated with minimum radius $R_{\min}$by differentiating 3.26,

$$D(R_{\min}) = \left(\frac{2 + (\gamma - 1)M^2}{\gamma + 1} \right)^{\frac{1}{\gamma - 1}} \tag{3.27}$$

With this known, one can find $R_{\min}$ as a function of the initial Mach number M_{ref} , and the use the same for various cases of Mach number, as shown by 3.2. Figure-3.2, gives a fairly good amount of idea, as how one must choose the parameters for the the cross section. In our analysis, for seeing the effect of varying cross-sectional boundary, we have kept the cross sectional area constant throughout the duct, though varying only the geometry of the same. A constant cross-sectional area effectively means that the mean flow density D_0, and hence also the Mach number M, will remain constant throughout the duct. Thus, on light of this set-up figure-3.2 holds good for the entire duct, and hence guiding us to maintain the 'slowly varying' nature of the duct. So with the situation of mean flow solved, one can proceed ahead towards dealing the acoustic perturbations, where the situation is not simple. While confronting the mean flow, we had used the methods of regular perturbation to get a good approximation of the mean flow parameters.But, for the acoustic perturbations, the asymptotic methods summoned to solve the acoustic profile will be from that of multiple scales method.

Chapter 4

Acoustic perturbations

4.1 The Duct Modes

Before we jump into the rigours of dealing with slowly varying ducts, a little background into the acoustic perturbations in a straight duct would provide us with a good starting point. We assume for simplicity, that we have a uniform mean flow at our bidding. Which implies the axial mean velocity v_0, mean pressure p_0, density ρ_0, and sound speed c_0, are constants throughout the ducts. This will transform the equations 2.21, 2.22, and 2.23, into

$$(i\omega + v_0 \frac{\partial}{\partial x})\hat{\rho} + \rho_0 \nabla \cdot \hat{\boldsymbol{v}} = 0 \tag{4.1a}$$

$$\rho_0(i\omega + v_0 \frac{\partial}{\partial x})\hat{\boldsymbol{v}} + \nabla \hat{p} = 0 \tag{4.1b}$$

$$(i\omega + v_0 \frac{\partial}{\partial x})(\hat{p} - c_0^2 \hat{\rho}) = 0 \tag{4.1c}$$

We now have an homentropic and an irrotational situation, and hence we have $\hat{\boldsymbol{v}} = \nabla \hat{\phi}$. Thus 4.1a becomes,

$$(i\omega + v_0 \frac{\partial}{\partial x})\hat{\rho} + \rho_0 \nabla^2 \hat{\phi} = 0 \tag{4.2}$$

With divergence operator applied on 4.1b, and using equations 4.1a, and 4.1c, we can eliminate $\hat{\phi}$, and $\hat{\rho}$, to obtain a convected reduced wave equation for the pressure

$$c_0^2 \nabla^2 \hat{p} - (i\omega + v_0 \frac{\partial}{\partial x})^2 \hat{p} = 0 \tag{4.3}$$

Now if one assumes that there is no mean flow, implying $v_0 = 0$, 4.3 reduces to the Helmholtz equation, with $c_0 = 1$

$$\nabla^2 \hat{p} + \omega^2 \hat{p} = 0 \tag{4.4}$$

21

With the absence of mean flow, and the straightness of the duct, one can do a Fourier transform in along the x direction, i.e. we can write pressure $\hat{p}$ as

$$\hat{p} = \tilde{p}\exp(-\mathrm{i}\kappa x) \tag{4.5}$$

where, κ, is the axial wave number. Thus further reducing 4.4 to

$$\nabla^2\tilde{p} + \alpha^2\tilde{p} = 0 \tag{4.6}$$

With $\kappa = f(\alpha)$. Now the eigenfunctions of the Helmholtz equation 4.6 are nothing but Fourier transformed solution of 4.4, and are referred to as modes, and they are self similar too in nature.

When we have a mean flow4.3 can be solved also in a similar manner, but with some special care taken to avoid any singular edge behaviour. It can be Fourier transformed in to an ordinary reduced wave equation

$$c_0(X)^2\nabla^2\tilde{p} + \zeta^2\tilde{p} = 0 \tag{4.7}$$

by introducing

$$\hat{p} = \tilde{p}(X, r, \theta; \zeta)\exp(-\mathrm{i}\frac{\zeta M}{c_0}X) \tag{4.8}$$

where $x = \beta X$, $\omega = \beta\zeta$, $M = \frac{v_0}{c_0}$, $\beta = \sqrt{1 - M^2}$. Thus one can see that even with the existence of mean flow one can represent the acoustic profile as Fourier transformed modes. But, that's where the ease ends of using the above analysis for studying acoustic profile, as we now have slowly varying duct profile. But by using the term of 'slowly varying' to a good effect, we can make some assumptions about the nature of the solution, and try to approximate the solution as it was done using Fourier transforms in the above cases.

4.2 Method of Multiple Scales: The WKB method

For dealing with acoustic perturbation, we must now focus on the equation, 2.32. Approximating equation 2.32, to the first order term of density ρ_0, using equation 2.13, and applying, $\boldsymbol{v}_0 = U_0\boldsymbol{e}_x + \boldsymbol{V}_\perp$, the following is obtained;

$$
\begin{aligned}
&\frac{1}{D_0(X)}\left[\frac{\partial}{\partial x} + \nabla_\perp\right] \cdot \left(D_0(X)\left[\frac{\partial}{\partial x} + \nabla_\perp\right]\hat{\phi}\right) \\
&- \left(\mathrm{i}\omega + (U_0\boldsymbol{e}_x + \boldsymbol{V}_\perp) \cdot \left[\frac{\partial}{\partial x} + \nabla_\perp\right]\right)\left\{\frac{1}{C_0^2}\left(\mathrm{i}\omega + (U_0\boldsymbol{e}_x + \boldsymbol{V}_\perp) \cdot \left[\frac{\partial}{\partial x} + \nabla_\perp\right]\right)\hat{\phi}\right\} = 0
\end{aligned}
\tag{4.9}
$$

Where, $C_0(X)$, is the first order approximation of the mach number c_0, as from equations 2.16, and 3.9, one can write, $c_0 = C_0 + \mathcal{O}(\epsilon^2)$. As the first order approximations of both

pressure and density are functions of the slow variable X, it is clear that, $C_0 = C_0(X)$. Equation 4.9, can be further modified using equation 3.4, and 3.12, and the following result can be obtained;

$$\nabla_\perp^2 \hat{\phi} + \hat{\phi}_{xx} + \epsilon \frac{1}{D_0(X)} \hat{\phi}_x D_{0X} - \frac{1}{C_0^2} \left[-\omega^2 \hat{\phi} + \mathrm{i}\omega U_0 \hat{\phi}_x + \epsilon \mathrm{i}\omega (\boldsymbol{V}_{\perp 0} \cdot \nabla_\perp) \hat{\phi} \right]$$
$$- \left[\frac{1}{C_0^2} \mathrm{i}\omega U_0 \hat{\phi}_x + \epsilon (U_0/C_0^2)_X \hat{\phi}_x + \frac{U_0^2}{C_0^2} \hat{\phi}_{xx} + \epsilon \frac{U_0}{C_0^2} (\boldsymbol{V}_{\perp 0} \cdot \nabla_\perp) \hat{\phi}_x + \epsilon \mathrm{i}\omega U_0 \hat{\phi}_x (1/C_0^2)_X \right]$$
$$- \frac{1}{C_0^2} \left[\epsilon U_0 (\boldsymbol{V}_{\perp 0} \cdot \nabla_\perp) \hat{\phi}_x + \epsilon \mathrm{i}\omega (\boldsymbol{V}_{\perp 0} \cdot \nabla_\perp \hat{\phi}) \right] + \mathcal{O}(\epsilon^2) = 0 \tag{4.10}$$

Which can be further written in a nice form by grouping the terms of the same order.

When we have a straight duct, we have modes as solutions. But with the duct deformed a little bit, it is reasonable to assume (from well-posedness of the problem leading to continuity of the solution) that solutions exist that are slightly deformed modes, a.k.a. slowly varying modes. This forms the basis of the WKB-Ansatz, which is taken for solving equation 4.10.

$$\hat{\phi} = \Psi(X, r, \theta; \epsilon) \exp\left(-\mathrm{i} \int^x \mu(\epsilon\xi; \epsilon) \,\mathrm{d}\xi\right) \tag{4.11a}$$

$$\hat{\phi}_x = (-\mathrm{i}\mu\Psi + \epsilon\Psi_X) \exp\left(-\mathrm{i} \int^x \mu(\epsilon\xi; \epsilon) \,\mathrm{d}\xi\right) \tag{4.11b}$$

$$\hat{\phi}_{xx} = (-\mu^2\Psi - \mathrm{i}\epsilon\mu_X\Phi - 2\mathrm{i}\mu\Psi_X + \epsilon^2\Psi_{XX}) \exp\left(-\mathrm{i} \int^x \mu(\epsilon\xi; \epsilon) \,\mathrm{d}\xi\right) \tag{4.11c}$$

such that regular expansions exist in ϵ for $\Psi(X, r, \theta; \epsilon)$ and $\mu(X; \epsilon)$, the axial wave number. Substituting equations 4.11a, 4.11b, and 4.11c, in equation, 4.10, grouping the terms of similar powers of ϵ, and putting $\Omega = \omega - \mu U_0$, one gets;

$$\nabla_\perp^2 \Psi + \left(\frac{\Omega^2}{C_0^2} - \mu^2\right) \Psi = \frac{\mathrm{i}\epsilon}{D_0\Psi} \left[\left[\left(\frac{\Omega U_0}{C_0} + \mu\right) D_0\Psi^2 \right]_X + \nabla_\perp \cdot \left(\frac{\Omega D_0}{C_0^2} \Psi^2 \boldsymbol{V}_{\perp 0}\right) \right] + \mathcal{O}(\epsilon^2) \tag{4.12}$$

Now expanding Ψ, and μ in the usual way;

$$\Psi(X, r, \theta; \epsilon) = \Psi_0(X, r, \theta) + \epsilon\Psi_1(X, r, \theta) + \mathcal{O}(\epsilon^2), \quad \mu(X; \epsilon) = \mu(X) + \mathcal{O}(\epsilon^2) \tag{4.13}$$

substituting in equation 4.12, and approximating till the leading order one gets;

$$\nabla_\perp^2 \Psi_0 + \left(\frac{\Omega^2}{C_0^2} - \mu^2\right) \Psi_0 = 0 \tag{4.14}$$

23

4.3 The Boundary Condition

According to [8] the acoustic boundary condition of an impedance wall along a curved wall with mean flow is;

$$i\omega(\hat{\boldsymbol{v}} \cdot \boldsymbol{n}) = [i\omega + \boldsymbol{v}_0 \cdot \nabla - \boldsymbol{n} \cdot (\boldsymbol{n} \cdot \nabla \boldsymbol{v}_0)]\left(\frac{\hat{p}}{Z}\right) \tag{4.15}$$

Where $\boldsymbol{v}$, is the original flow.
Now the domain of interest consists of a duct with arbitrary cross-section, slowly varying in the axial direction, as $f(X, r, \theta) = 0$, on the surface. Consider in cylindrical coordinates, the duct to be given by the function;

$$f(X, r, \theta) = r - R(X, \theta) = 0 \tag{4.16}$$

on the duct surface, the gradient is given by;

$$\nabla f = -\epsilon \boldsymbol{e}_x R_X + \boldsymbol{e}_r - \frac{1}{R} R_\theta \boldsymbol{e}_\theta \tag{4.17}$$

The vector normal to the surface is given by;

$$\boldsymbol{n} = \frac{\nabla f}{|\nabla f|} \tag{4.18}$$

while the transverse gradient $\nabla_\perp f$;

$$\nabla_\perp f = \boldsymbol{e}_r - \boldsymbol{e}_\theta \frac{1}{R} R_\theta \tag{4.19}$$

$\boldsymbol{n}_\perp = \nabla_\perp f/|\nabla_\perp f|$ denotes the component of the surface-normal vector $\boldsymbol{n}$ in the plane of a cross section. Thus $\boldsymbol{n}$, can be written in an approximate form as;

$$\boldsymbol{n} = \frac{\nabla f}{|\nabla_\perp f|} + \mathcal{O}(\epsilon^2) = \boldsymbol{n}_\perp - \epsilon \frac{R R_X}{\sqrt{R^2 + R_\theta^2}} \boldsymbol{e}_x + \mathcal{O}(\epsilon^2) \tag{4.20}$$

For an homentropic, irrotational flow, its known that, $\hat{\boldsymbol{v}} = \nabla \hat{\phi}$. Therefore, 4.15 can be written in terms of the potential also. Using 3.4, 4.20, in 4.15 yields;

$$i\omega(\boldsymbol{n}_\perp \cdot \nabla_\perp \Psi) - \epsilon \omega \mu \frac{R R_X}{\sqrt{R^2 + R_\theta}} \Psi = [i\omega + \boldsymbol{v}_0 \cdot \nabla - \boldsymbol{n} \cdot (\boldsymbol{n} \cdot \nabla \boldsymbol{v}_0)]\left(\frac{\hat{p}}{Z}\right) \tag{4.21}$$

Now pressure again can be written in the form of a WKB Ansatz, as follows;

$$\hat{p} = -D_0(i\Omega \Psi + \epsilon U_0 \Psi_X + \epsilon \boldsymbol{V}_{\perp 0} \cdot \Psi) \exp\left(i \int^x \mu(\epsilon \xi; \epsilon) d\xi\right) \tag{4.22}$$

24

Substituting [4.22](#), in [4.21](#), the following result is obtained;

$$i\omega(\boldsymbol{n}_\perp \cdot \nabla_\perp \Psi) - \epsilon\omega\mu\frac{RR_X}{\sqrt{R^2 + R_\theta}}\Psi = \frac{\Omega^2 D_0}{Z}\Psi$$

$$- i\epsilon\left[U_0\left(\frac{D_0\Omega\Psi}{Z}\right)_X + U_0\frac{D_0\Omega}{Z}\Psi_X + D_0\Omega\boldsymbol{V}_{\perp 0}\cdot\nabla_\perp\left(\frac{\Psi}{Z}\right)\right]$$

$$+ i\epsilon\left[-\frac{D_0\Omega}{Z}\boldsymbol{V}_{\perp 0}\cdot\nabla_\perp\Psi + \boldsymbol{n}_\perp\cdot(\boldsymbol{n}_\perp\cdot\nabla_\perp\boldsymbol{V}_{\perp 0})\frac{D_0\Omega\Psi}{Z}\right] \quad (4.23)$$

Using the asymptotic expansion of Ψ, in the above equation, and considering only the leading order terms;

$$i\omega(\boldsymbol{n}_\perp \cdot \nabla_\perp \Psi_0) - \frac{\Omega^2 D_0}{Z}\Psi_0 = 0 \quad r = R \tag{4.24}$$

4.4 The Unknown Amplitude

The detailed derivation for amplitude $N(X)$, is given by Rienstra-[3].The leading order term as given by [4.24](#), can be written as $\Psi_0 = N(X)\psi_n(X, r, \theta)$. Where $N(X)$, is the unknown amplitude yet to be found out. Thus the main equation for obtaining the eigen-modes becomes;

$$-\nabla_\perp\psi = \alpha^2\psi, \quad \text{with} \quad (\boldsymbol{n}_\perp \cdot \nabla_\perp\psi) = \frac{\Omega^2 D_0}{i\omega Z}\psi \text{ at } r = R \tag{4.25}$$

with

$$\Omega^2 - \frac{(\omega - \Omega)^2}{M^2} = \alpha^2 \quad M = \frac{U_0}{C_0} \tag{4.26}$$

The ψ_n can be obtained by normalizing the solution of [4.25](#), as

$$\psi = \frac{\psi}{\iint_A \psi^2 dS} \tag{4.27}$$

For determining the amplitude, $N(X)$, one must go forward into order of Ψ_1, for getting its solvability condition. From equation, [4.12](#) one can get the equation, related to $\mathcal{O}(\epsilon)$ as;

$$\nabla_\perp^2\Psi_1 + \alpha^2\Psi_1 = \frac{i}{D_0\Psi_0}\left[\left[\left(\frac{\Omega U_0}{C_0} + \mu\right)D_0\Psi_0^2\right]_X + \nabla_\perp\cdot\left(\frac{\Omega D_0}{C_0}\Psi_0^2\boldsymbol{V}_{\perp 0}\right)\right] \tag{4.28}$$

The boundary condition corresponding to $\mathcal{O}(\epsilon)$,

$$i\omega(\boldsymbol{n}_\perp\cdot\nabla_\perp\Psi_1) - \frac{\Omega^2 D_0}{Z}\Psi_1 = \omega\mu\frac{RR_X}{\sqrt{R^2 + R_\theta^2}}\Psi_0 - i\left[U_0\left(\frac{D_0\Omega\Psi_0}{Z}\right)_X + U_0\frac{D_0\Omega}{Z}\Psi_{0,X}\right]$$

$$- i\left[D_0\Omega\boldsymbol{V}_{\perp 0}\cdot\left(\frac{\Psi_0}{Z}\right) + \frac{D_0\Omega}{Z}\boldsymbol{V}_{\perp 0}\cdot\nabla_\perp\Psi_0\right] + i\boldsymbol{n}_\perp\cdot(\boldsymbol{n}_\perp\cdot\nabla_\perp\boldsymbol{V}_{\perp 0})\frac{D_0\Omega\Psi_0}{Z} \tag{4.29}$$

Multiplying 4.12 with $D_0\Psi_1$, and 4.29 with $D_0\Psi_0$, and then integrating the difference over a cross-section A to obtain;

$$D_0 \iint_A (\Psi_0 \nabla_\perp^2 \Psi_1 - \Psi_1 \nabla_\perp^2 \Psi_0)\,\mathrm{d}S = \mathrm{i} \iint_A \left[\left(\frac{\Omega U_0}{C_0^2} \right) + \mu \right) D_0 \Psi_0^2 \right]_X \mathrm{d}S$$
$$+ \mathrm{i} \iint_A \nabla_\perp \cdot \left(\frac{\Omega D_0}{C_0^2} \Psi_0^2 \boldsymbol{V}_{\perp 0} \right) \mathrm{d}S \qquad (4.30)$$

For the first integral in the right hand side, we use the Leibnitz rule, and we get the following expression;

$$\iint_A \left[\left(\frac{\Omega U_0}{C_0^2} + \mu \right) D_0 \Psi_0^2 \right]_X = \left[\left(\frac{\Omega U_0}{C_0^2} \right) + \mu \right) D_0 \iint_A \Psi_0^2 dS \right] - \left(\frac{\Omega U_0}{C_0^2} + \mu \right) D_0 \int_0^{2\pi} \Psi_0^2|_{r=R} R R_X \mathrm{d}\theta$$
$$(4.31)$$

The second integral can be manipulated as follows;

$$\iint_A \nabla_\perp \cdot \left(\frac{\Omega D_0}{C_0^2} \Psi_0^2 \boldsymbol{V}_{\perp 0} \right) \mathrm{d}S = \frac{\Omega D_0}{C_0^2} \int_{\partial A} \Psi_0^2 (\boldsymbol{V}_{\perp 0} \cdot \boldsymbol{n})\,\mathrm{d}l$$
$$= \frac{\Omega D_0}{C_0^2} \int_0^{2\pi} \Psi_0^2|_{r=R} (\boldsymbol{V}_{\perp 0} \cdot \boldsymbol{n}) \sqrt{(R^2 + R_\theta^2)}\,\mathrm{d}\theta$$
$$= \frac{\Omega D_0 U_0}{C_0^2} \int_0^{2\pi} \Psi_0^2|_{r=R} R R_X \mathrm{d}\theta \qquad (4.32)$$

Together which yields,

$$D_0 \iint_A (\Psi_0 \nabla_\perp^2 \Psi_1 - \Psi_1 \nabla_\perp^2 \Psi_0)\,\mathrm{d}S = \mathrm{i} \left[\left(\frac{\Omega U_0}{C_0^2} \right) + \mu \right) D_0 \iint_A \Psi_0^2\,\mathrm{d}S \right] - \mathrm{i}\mu D_0 \int_0^{2\pi} \Psi_0^2|_{r=R} R R_X\,\mathrm{d}\theta$$
$$(4.33)$$

Using the boundary conditions for Ψ_0 and Ψ_1, then the following expression

$$D_0 \int_{\partial A} [\Psi_0 (\boldsymbol{n} \cdot \nabla_\perp \Psi_1) - \Psi_1 (\boldsymbol{n} \cdot \nabla_\perp \Psi_0)]\mathrm{d}l =$$
$$- \frac{D_0}{\omega} \int_{\partial A} \left[U_0 \Psi_0 \left(\frac{D_0 \Omega}{Z} \right) \Psi_0)_X + \frac{U_0 D_0 \Omega}{Z} \Psi_0 \Psi_{0,X} \right] \mathrm{d}l$$
$$- \frac{D_0}{\omega} \int_{\partial A} \left[\frac{D_0 \Omega}{Z} \Psi_0 (\boldsymbol{V}_{\perp 0} \cdot \nabla_\perp \Psi_0) - \boldsymbol{n} \cdot (\boldsymbol{n} \cdot \boldsymbol{V}_{\perp 0}) \frac{\Psi_0^2 D_0 \Omega}{Z} \right] \mathrm{d}l$$
$$- \mathrm{i}\mu D_0 \int_0^{2\pi} \Psi_0^2|_{r=R} R R_X \mathrm{d}\theta \quad (4.34)$$

26

Combining 4.33, and 4.34, and using the fact the impedance wall is non-porous, i.e $\boldsymbol{V} \cdot \boldsymbol{n} = 0$, we obtain;

$$i\omega \left[\left(\frac{\Omega U_0}{C_0^2} + \mu \right) D_0 N^2 \right]_X = \int_{\partial A} \epsilon^{-1} \mathcal{M} \left(\frac{\Omega D_0^2 \Psi_0^2}{Z} \boldsymbol{V} \right) \mathrm{d}l + \mathcal{O}(\epsilon^2) \qquad (4.35)$$

where $\mathcal{M}$, is an operator given by;

$$\mathcal{M}(\boldsymbol{f}) = \nabla \cdot \boldsymbol{f} - \boldsymbol{n} \cdot (\boldsymbol{n} \cdot \nabla \boldsymbol{f}) \qquad (4.36)$$

Now using the lemma stated and proved in Rienstra-[3], the following relation for the unknown amplitude is obtained as follows,

$$\frac{Q^2}{N^2} = \frac{\omega \sigma D_0}{C_0} + \frac{D_0^2 \Omega}{i\omega} U_0 \int_{\partial A} \frac{1}{Z} \psi_n^2 \mathrm{d}l \qquad (4.37)$$

Where $\sigma = \sqrt{1 - (C_0^2 - U_0^2)\frac{\alpha^2}{\omega^2}}$, is the reduced axial wave number, and Q, is a suitable integration constant.

Chapter 5

The Numerical Solution

5.1 The Motivation

Equation 4.25, combined with 4.26, is a non-linear eigenvalue problem, which for domains, like circle, and square can be solved analytically, but when demand arises for solving the equation for solving different boundary structures, one has to resort to numerical solution. The problem is linearly elliptic in ψ, whereas it is non-linear when the matter comes to finding in the eigenvalues, as the boundary condition depends on the eigenvalue in a non-linear way. Its clear, that one has to use an iterative method for solving such problems, and without exception, our main aim is to solve the problem, by solving a linear eigenvalue problem of type;

$$-\nabla_\perp^2 \psi = \lambda \psi, \quad \boldsymbol{x} \in A, \quad \text{with} \quad \boldsymbol{n} \cdot \nabla \psi = \frac{\Omega}{\mathrm{i}\omega Z}\psi \quad \text{on} \quad \partial A \tag{5.1}$$

Equation 4.25, can be solved analytically for certain geometries using the method of separation of variables, e.g. circle, and rectangle. But for an arbitrary geometry, it becomes difficult to solve for the equation. Thus an iterative numerical method based on 5.1 is sought to solve the problem. On one hand we have the usual methods like the Finite Difference Method, and the Finite Element method, on the other we have the Boundary Integral Method. [17] gives us a way of approximating the eigenfunctions as a boundary integral of certain special functions. A curious case to note, is the complexity involved in solving such boundary integral for 2-D geometry, where the eigenfunctions can be represented as a boundary integral of Hankel functions. Whereas, for a 3-D geometry the same is represented as a boundary integral of simple exponential functions. This implies that for solving the acoustic pressure, one needs to generate Hankel functions for every cross-sectional area under consideration, which might be time consuming to formulate on the computer.

With the geometry being arbitrary, it is but a natural choice to take the help of FEM rather than FDM. The routine scientific computing software, MATLAB takes a back seat, when it comes in using FEM, involving complex numbers as inputs. Another option was to use

COMSOL, but it too had its reservations in using complex inputs. FORTRAN on which numerous numerical experiments run was ruled out, as time will be consumed in coding of the entire problem. Thus amongst numerous FEM softwares available, the searched zeroed down to Freefem++, which happens to be a software developed on C++, by Pirroneau and his team from France. The biggest advantage of using Freefem++, other than it being an free software, it comes built in with many a C++ libraries to deal with vectors, matrix, etc of complex numbers. It has a built in Eigenvalue problem solver which is based on the Krylov space methods. Also, it can be programmed without using any GUI, in any text editor. To start with, one must know the weak form of the given equation to solve a problem using Freefem++. The Freefem++ allows 3 major advantages for ease of calculation, and also for accurate approximation, viz. a built-in eigenvalue solver, a built-in algorithm for calculating the integrals of many functions over the given geometry, and last but not the least, a wide variety of finite element basis functions. Also the visualization also is easy with paraview, and other such open-source softwares.

Given, the demands of Freefem++, the weak form of 5.1 is,

$$\iint_A \nabla\psi\nabla\zeta \, \mathrm{d}S - \iint_A \lambda\psi\zeta \, \mathrm{d}S - \int_{\partial A} \frac{\Omega}{\mathrm{i}\omega Z}\psi\zeta \, \mathrm{d}l = 0 \tag{5.2}$$

Where, ψ, and ζ, belong to appropriate spaces as required. Thus, armed with the arsenal of Freefem++, we go about constructing numerical scheme for solving the non-linear eigenvalue problem at hand. And, to start with we consider, $D_0 = 1$, and by considering a single cross-section. The two major iterative methods, discussed here are as follows;

1. Simple Iteration Method

2. Newton Iteration Method

Equation, 4.25, has many parameter space, to span in terms of impedance Z, the Mach number M. Suitable limiting cases for all these three parameters form, starting points for the techniques listed above. Each limiting case, yields a separate boundary condition, which will be listed as follows;

1. For impedance, $Z = \infty$, 4.25, translates into

$$-\nabla_\perp\psi = \alpha^2\psi, \ \boldsymbol{x} \in \ A \quad \text{with} \quad (\boldsymbol{n}_\perp \cdot \nabla_\perp\psi) = 0 \ \text{ on } \ \partial A \tag{5.3}$$

2. For impedance, $Z = 0$, 4.25, translates into;

$$-\nabla_\perp\psi = \alpha^2\psi, \ \boldsymbol{x} \in \ A \quad \text{with} \quad (\psi) = 0 \text{ on } \partial A \tag{5.4}$$

3. For Mach number $M = 0$, 4.25 translates into;

$$-\nabla_\perp\psi = \alpha^2\psi, \ \boldsymbol{x} \in \ A \quad \text{with} \quad (\boldsymbol{n}_\perp \cdot \nabla_\perp\psi) = \frac{\omega}{\mathrm{i}Z}\psi \text{ on } \partial A \tag{5.5}$$

29

Equations 5.3,5.4, and 5.5, are starting points used for starting the iteration process, at the fan end of the duct.For solving the problem for other cross-sections the starting point is obtained from the parameters obtained from previous cros section.The iterative solvers created, iterate upon a single eigenvalue and the results, obtained correspond to the same eigenvalue. The Eigenvalue PDE, was solved using an Open source Finite Element software Freefem++.

5.2 The numerical methods

5.2.1 The simple iteration method

Taking motivation from, 4.26, one can write $\Omega = g(\alpha)$. Let, α_n, denote the nth, eigenvalue of the Laplace operator, obtained numerically. Let Ω^m, and α_n^m, denote the mth iterated values of Ω, and α. Then the following iteration algorithm can be created;

Algorithm: Simple iteration method

1. Consider α_n^0, as starting value obtained from 5.3, 5.4, or 5.5

2. $\Omega_m^0 = g(\alpha_n^0)$

3. While (error > tol)
   Do

   (a) Solve

   $$-\nabla_\perp \psi = (\alpha^m)^2 \psi, \quad \text{with} \quad (\boldsymbol{n}_\perp \cdot \nabla_\perp \psi) = \frac{(\Omega^{m-1})^2 D_0}{i\omega Z} \psi \text{ on } \partial A \qquad (5.6)$$

   (b) $\Omega^m = g(\alpha^m)$
   (c) error=$|\Omega^m - \Omega^{m-1}|$

4. END

5.2.2 The Newton's method

The Newton's method, involves putting 4.25,and 4.26 in a more abstract setting as follows;

$$-\nabla^2 \psi = Q(\lambda)\psi \quad \text{for} \quad \boldsymbol{x} \in \mathcal{A}, \quad \text{with} \quad (\boldsymbol{n} \cdot \nabla\psi) = R(\lambda)\psi \quad \text{at} \quad \boldsymbol{x} \in \partial\mathcal{A} \qquad (5.7)$$

where Q, and R, are given (smooth) functions of parameter $\lambda \in \mathbb{C}$. The main aim is to find the sequence (λ_n, ψ_n), of eigenvalues and eigenfunctions. For solving, 5.7, this method resorts in solving an equivalent problem, given by;

$$-\nabla^2 \psi = q\psi \quad \text{for} \quad \boldsymbol{x} \in \mathcal{A}, \quad \text{with} \quad (\boldsymbol{n} \cdot \nabla\psi) = R(k)\psi \quad \text{at} \quad \boldsymbol{x} \in \partial\mathcal{A} \qquad (5.8)$$

With, k given, $R(k)$, is known. 5.8 becomes now a standard eigenvalue problem, and thus one can write, $q = q(k)$. Taking motivation, from 5.7, and 5.8, the main problem reduces in finding $k = \lambda_n$ such that;

$$Q(k) - q(k) = 0 \tag{5.9}$$

A Newton iteration of this equation would be given by the sequence k_m iteratively defined as follows;

$$k_{m+1} = k_m - \frac{Q_m - q_m}{Q'_m - q'_m} \tag{5.10}$$

where $Q_m = Q(k_m)$, and $q_m = q(k_m)$. It is conjectured that k_m, converge to an eigenvalue λ, of the original problem 5.7.

For a successful implementation of this iteration, one has to find out the derivative of q. Consider, two solutions to problem 5.8, say, (k_1, q_1, R_1, ϕ_1), and (k_2, q_2, R_2, ϕ_2), and combine them as follows;

$$\phi_1(\nabla^2\phi_2 + q_2\phi_2) - \phi_2(\nabla^2\phi_1 + q_1\phi_1) = 0 \tag{5.11}$$

$$\nabla \cdot (\phi_1\nabla\phi_2 - \phi_2\nabla\phi_1) + (q_2 - q_1)\phi_1\phi_2 = 0 \tag{5.12}$$

$$\iint_{\mathcal{A}} \left[\nabla \cdot (\phi_1\nabla\phi_2 - \phi_2\nabla\phi_1) + (q_2 - q_1)\phi_1\phi_2\right] \mathrm{d}\boldsymbol{x} = 0 \tag{5.13}$$

$$\int_{\partial\mathcal{A}} \left[\phi_1(\boldsymbol{n} \cdot \nabla\phi_2) - \phi_2(\boldsymbol{n} \cdot \nabla\phi_1)\right] \mathrm{d}l + (q_2 - q_1)\iint_{\mathcal{A}} \phi_1\phi_2 \, \mathrm{d}\boldsymbol{x} = 0 \tag{5.14}$$

$$(R_2 - R_1)\int_{\partial\mathcal{A}} \phi_1\phi_2 \, \mathrm{d}l + (q_2 - q_1)\iint_{\mathcal{A}} \phi_1\phi_2 \, \mathrm{d}\boldsymbol{x} = 0 \tag{5.15}$$

$$\frac{(R_2 - R_1)}{k_2 - k_1}\int_{\partial\mathcal{A}} \phi_1\phi_2 \, \mathrm{d}l + \frac{(q_2 - q_1)}{k_2 - k_1}\iint_{\mathcal{A}} \phi_1\phi_2 \, \mathrm{d}\boldsymbol{x} = 0 \tag{5.16}$$

Taking limit as $k_2 \to k_1$, 5.16 becomes;

$$R'(k_1)\int_{\partial\mathcal{A}} \phi_1^2 \, \mathrm{d}l + q'_1(k_1)\iint_{\mathcal{A}} \phi_1^2 \, \mathrm{d}\boldsymbol{x} = 0 \tag{5.17}$$

or in general

$$q'(k) = -R'(k)\frac{\int_{\partial\mathcal{A}} \phi^2 \, \mathrm{d}l}{\iint_{\mathcal{A}} \phi^2 \, \mathrm{d}\boldsymbol{x}} \tag{5.18}$$

Concretizing the abstract setting to suit the concerning problem;

$$\lambda = \Omega, \ Q(\lambda) = \lambda^2 - \frac{(\omega - \lambda)^2}{M^2}, \ R(\lambda) = \frac{\lambda^2}{i\omega Z}, \ Q'(\lambda) = 2\lambda + \frac{2(\omega - \lambda)}{M^2}, \ R'(\lambda) = \frac{2\lambda}{i\omega Z}. \tag{5.19}$$

The axial wave number is then

$$\mu = \frac{\omega - \lambda}{M}$$

31

Algorithm:- The Newton's Method

1. Solve for α_n^0, using 5.3, 5.4, or 5.5

2. $\Omega_n^0 = \lambda_n^0 = g(\alpha_n^0)$

3. while (error > tol)
   Do

   (a) $Q_m = Q(\lambda_n^m)$, $R_m = R(\lambda_n^m)$
   (b) Solve

   $$-\nabla^2\psi = q\psi \quad \text{for} \quad \boldsymbol{x} \in \mathcal{A}, \quad \text{with} \quad (\boldsymbol{n}\cdot\nabla\psi) = R(k)\psi \quad \text{at} \quad \boldsymbol{x} \in \partial\mathcal{A} \quad (5.20)$$

   to get eigenvalue, q_n^m, and eigenfunction ϕ_n^m
   (c) Obtain $q'(\lambda_n^m)$, as given by 5.18
   (d) Solve 5.10 to get λ_n^{m+1}
   (e) error=$|\Omega^m - \Omega^{m-1}|$

4. END

The axial wave number μ, helps us in identifying the left and the right running modes. If, $\text{Im}(\mu) < 0$ then we have a right running mode, and if $\text{Im}(\mu) > 0$, then the mode is left running.

5.3 Analysis of the Numerical Solutions

5.3.1 Performance of numerical methods

Problem, 4.25, along with the condition 4.26, can be solved analytically for certain geometries like, circle, and rectangle. For numerically solving the problem, finite element method was utilized, and Freefem++ software was used to solve the same. In order to test the numerical methods discussed in the previous section, the geometry of circle was considered, for which analytical solution exists. The solution to 4.25, for a circular geometry, of radius $r = 1$, can be obtained, by method of separation of variables, and is of the form;

$$\psi(r,\theta) = e^{-im\theta}\mathcal{J}_{m\alpha}(r) \quad (5.21)$$

where $\mathcal{J}_m$, denotes the Bessel function of order m, of the first kind, and m denotes the separation constant, which in turn refers to the radial axes of symmetry.
While applying the boundary condition at $r = 1$, the Bessel function $\mathcal{J}_m$, can be treated as a function of α, and yields the following relation;

$$\alpha\mathcal{J}_m'(\alpha) = \frac{\Omega^2(\alpha)}{i\omega Z}\mathcal{J}_m(\alpha) \quad (5.22)$$

α_n	Bessel $\mathcal{J}_m(m=)$	Simple $(Z=\infty)$	Newton $(Z=\infty)$	Simple $(M=0)$	Newton $(M=0)$
α_1	$1.2475 + 0.6073\mathrm{i}(m=0)$	$1.2477 + 0.6074\mathrm{i}$	$1.2476 + 0.6074\mathrm{i}$	$1.2476 + 0.6075\mathrm{i}$	$1.2475 + 0.6072\mathrm{i}$
α_3	$2.3303 + 0.5606\mathrm{i}(m=1)$	$2.3314 + 0.5611\mathrm{i}$	$2.3311 + 0.5611\mathrm{i}$	$2.331 + 0.5612\mathrm{i}$	$2.3311 + 0.5611\mathrm{i}$
α_5	$3.4647 + 0.5936\mathrm{i}(m=2)$	$3.4667 + 0.5951\mathrm{i}$	$3.4667 + 0.5948\mathrm{i}$	$3.4667 + 0.5947\mathrm{i}$	$3.4667 + 0.5948\mathrm{i}$
α_6	$4.0070 + 0.4148\mathrm{i}(m=0)$	$4.0115 + 0.4167\mathrm{i}$	$4.0115 + 0.4168\mathrm{i}$	$4.0115 + 0.4167\mathrm{i}$	$4.0015 + 0.4167\mathrm{i}$
α_7	$4.5224 + 0.7300\mathrm{i}(m=3)$	$4.5262 + 0.7322\mathrm{i}$	$4.9832 + 0.484\mathrm{i}$	$4.5264 + 0.7323\mathrm{i}$	$4.5262 + 0.7322\mathrm{i}$
α_9	$5.3388 + 0.4266\mathrm{i}(m=1)$	$5.3483 + 0.4289\mathrm{i}$	$5.73057 + 0.29119\mathrm{i}$	$5.3483 + 0.4290\mathrm{i}$	$5.3484 + 0.4290\mathrm{i}$

Table 5.1: Comparison of the eigenvalues, ($\omega = 4$, $M = 0.3$, and $Z = 2 + 1\mathrm{i}$)

where $\Omega = g(\alpha)$, which can be obtained by solving the relation given by 4.26.

Thus, the eigenvalues α_n, of the Laplace operator in 4.25, has to satisfy the above relation. This crucial relation, is used to counter-check the results obtained by numerical methods discussed in the previous section. Many a starting points discusses were put through the numerics, and were iterated upon for first 15 eigenvalues, with $M = 0.3$, $\omega = 4$, and $Z = 2 + 1\mathrm{i}$. Figures, 5.1a, 5.1b, 5.1c, and 5.1d, gives the plot of the eigenfunction, ϕ_9, corresponding to the eigenvalue, α_9. It can be seen that, there is only one axis of radial symmetry in the figures, thus $m = 1$. Now, one can compare the values of α_9, obtained using different methods, and the one obtained using relation 5.22.

Table-5.1, gives a comparative study of how the numerical methods performed, in approximating the eigenvalues. An interesting point to note, is regarding the Newton's method with starting point as $Z = \infty$. For initial few eigenvalues, the method gives a good approximation of the same, but for α_7, things go haywire, and the results obtained from the method starts deviating from the analytical ones. Though, figure-5.1b gives a a profile with radial symmetry of $m = 2$, one can clearly see from the table that the obtained eigenvalues don't match at all with the theoretically obtained ones using the Bessel functions. Its slow competitor, the simple iterator, surprisingly gives a very good approximation for many eigenvalues. The same kind of divergence, with regards to the eigenvalues was observed in the Newton iteration, whose starting point happened to be the case of $Z = 0$. The only exception, in case of the Newton's method was that with the starting point of $M = 0$. In this case, problem given by, 5.5 in the first iteration itself, which involves the value of Z, as given by the user. In this particular case, the Newton's method found a good match with the theoretical results obtained using Bessel's functions. On the other hand, it was found that the simple iterator found its mark every time, irrespective of the starting point. Therefore, a conclusion was made, that the span of parameter space for Newton's method is small compared to that of the simple iteration.

A sketchy reason fingering towards the starting iteration can be given for this anomaly in the Newton's method. Both the Newton, and the simple iterator, are fixed point methods. Lets denote the simple iterator by the following equation;

$$x = f(x) \tag{5.23}$$
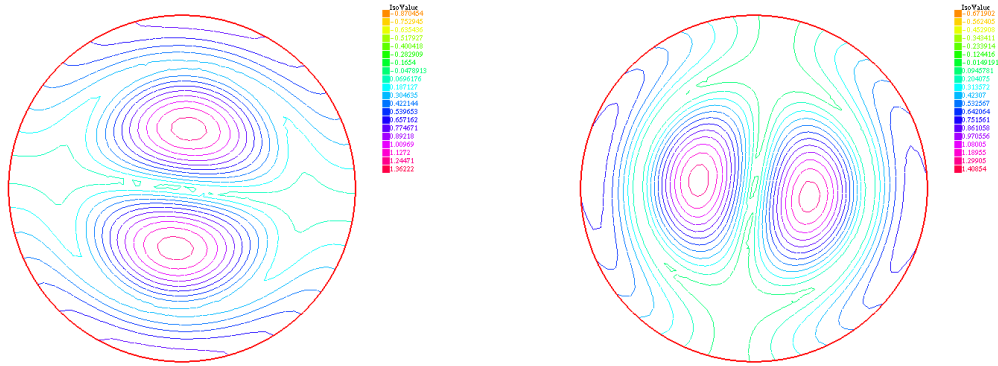
(a) Simple iteration, with $Z = \infty$ starting point

(b) Newton iteration, with $Z = \infty$ starting point
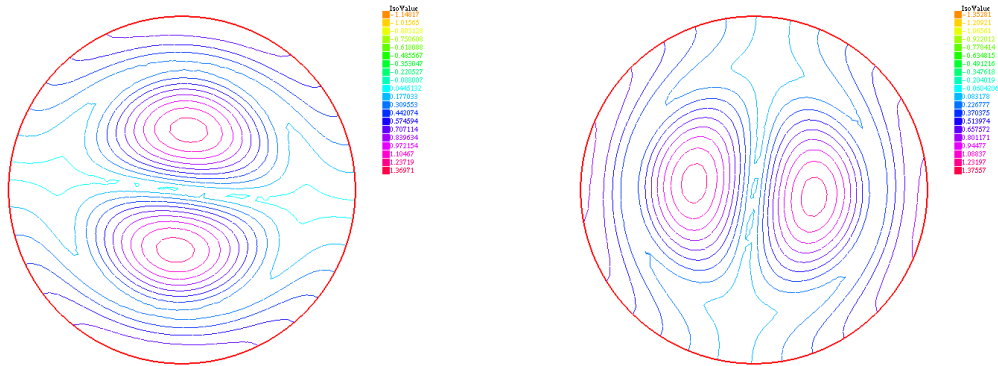
(c) Simple iteration, with $M = 0$ starting point

(d) Newton iteration, with $M = 0$ starting point

Figure 5.1: Plot of Eigenfunction, ϕ_9, corresponding to eigenvalue α_9 ($\omega = 4$, $M = 0.3$, $Z = 2 + 1i$)

Then the Newton's method can be denoted by;

$$x = F(x), \quad \text{where} \quad F(x) = \frac{f(x) - xf'(x)}{1 - f'(x)} \tag{5.24}$$

The Banach fixed point theorem dictates that, for a method to converge, $|g(x)| < 1$, where, $g(x) = f'(x)$, or $g(x) = F'(x)$, and for Newton's method $F'(x) = \frac{f-x}{(1-f')^2}f''$. The reason might be that, for simple iterator, $|f'(x)| < 1$, for all the starting iterations, whereas for the Newton's method $|F'(x)| < 1$, only for a few selected starting points, e.g, the one with $M = 0$. A further array of tests were planned in order to test the convergence, and the robustness of the simple iterative method with $Z = \infty$ as the starting point. The problem corresponding to $Z = 0$, is the eigenvalue problem given by 5.4. The exact solution for the

34

α_n	Bessel $\mathcal{J}_m$	Numerical Soution
n= 1	$2.4048(m = 0)$	$2.4057 + 1.021e - 10i$
n= 3	$3.8317(m = 1)$	$3.8353 + 9.3117e - 11i$
n= 5	$5.1356(m = 2)$	$5.1447 + 9.1511e - 11i$
n= 7	$6.3802(m = 3)$	$6.398 + 7.77e - 11i$
n= 9	$7.0156(m = 1)$	$7.0376 + 6.74e - 11i$
n=11	$7.5883(m = 4)$	$7.6192 + 5.79e - 11i$
n=13	$8.4172(m = 2)$	$8.4554 + 4.254e - 11i$
n=15	$8.6537(m = 0)$	$8.696 + 3.811e - 11i$

Table 5.2: Table of Eigenvalues obtained using simple iteration as $Z \to 0$ ($\omega = 3$, $M = 0.3$, and $Z = 1e - 10$)

equation is given by the 5.21, but the boundary condition at $r = 1$, yields the relation;

$$\mathcal{J}_m(\alpha) = 0 \tag{5.25}$$

Table-5.2, shows how the iteration models, converges to the case $Z = 0$.

All the above analysis was carried using the $P1$ basis function, i.e piecewise continuous and linear basis function. Now, we like see the effect of using different basis functions for sake of increasing accuracy. In our case, we have used the piecewise linear, and the piecewise quadratic element for doing the above analysis. Figure-5.2 gives an idea into the exactness of numerical solutions obtained by using different kinds of finite element basis functions. The main point to notice in this particular set-up is that, the P1 finite elements were able to give a close match for the starting few eigenvalues, but for higher eigenvalues, its not so accurate. Hence, keeping in the same parameters, a change to P2 basis functions was necessitated and then the problem was resolved for higher eigenvalues.

5.3.2 Surface wave analysis

The iteration techniques implemented above, show a fairly good match with the value calculated theoretically, using the Bessel functions, $\mathcal{J}_m$. In order to ascertain further the robustness of the iteration models, we increase the frequency, and try to locate the elusive surface waves. Surface waves are mechanical waves, which might be acoustic, or hydrodynamic, but as their name suggests they reside and propagate near the surface, and decay exponentially inside the given area. Surface waves are particularly difficult to find, therefore the main of this section is to locate the existence of surface wave, and interpret it in terms of the Lorentz transformed axial wave number σ. The surface waves mainly depend on the impedance Z of the attenuating wall.
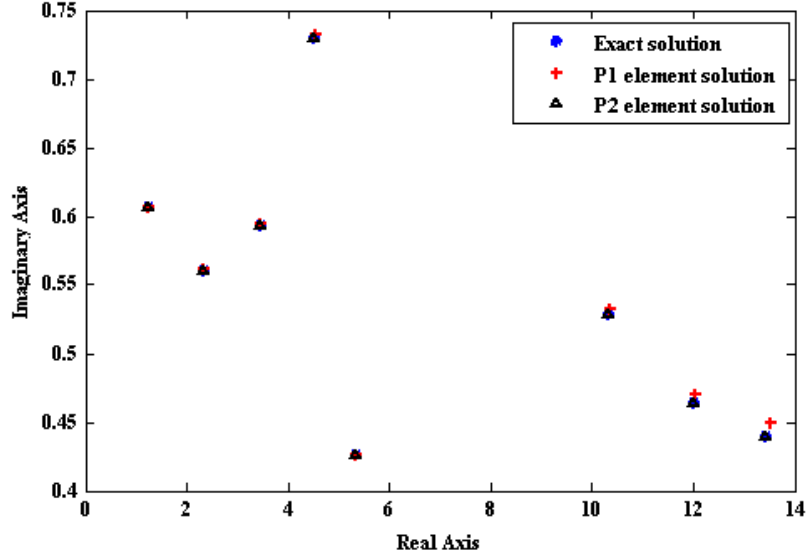
Figure 5.2: Effect of different finite element basis functions on the eigenvalues for $M = 0.3$, $Z = 2 + 1\mathrm{i}$, and $\omega = 4, 20$

The circular cross-section

To begin our quest of finding the surface waves, we consider the following Ansatz, that $\Omega = \mathcal{O}(\omega)$, and $\alpha = \mathcal{O}(\omega)$. Hence $\alpha = \beta\omega$, and $\Omega = \Gamma\omega$. Taking, $\epsilon = \frac{1}{\omega}$(this ϵ is different than the previous ones), and substituting the Ansatz in 4.25, and 4.26, we get in circular polar coordinates;

$$\epsilon^2 \left(\psi_{rr} + \frac{1}{r}\psi_r + \frac{1}{r^2}\psi_{\theta\theta} + \right) + \beta^2\psi = 0 \quad \text{in } \nu \tag{5.26a}$$

$$\text{with} \quad \epsilon\psi_r = \frac{\Gamma^2}{\mathrm{i}Z}\psi \quad \text{on } \partial\nu \tag{5.26b}$$

This hints to us the possibility of the existence of surface waves. The outer solution for 5.26, is simple obtained by neglecting the ϵ^2 term, which turns out to be the trivial $\psi_{out} = 0$. The presence of ϵ^2, in the highest order of derivative hints to us at an existence of a boundary layer, close to the wall surface, which implies that, we need to scale up in order to dig deeper into the profile of the surface waves. Since, the modes are considered symmetric in the θ direction, we scale up only in the radial direction as;

$$r = 1 - \epsilon\rho \tag{5.27}$$

36

With this scaling, 5.26 becomes;

$$\left(\psi_{\rho\rho} - \frac{\epsilon}{(1-\epsilon\rho)}\psi_\rho + \frac{\epsilon^2}{(1-\epsilon\rho)^2}\psi_{\theta\theta} \right) + \beta^2\psi = 0 \tag{5.28a}$$

$$\psi_\rho = \frac{\mathrm{i}\Gamma^2}{Z}\psi \tag{5.28b}$$

with ϵ small one can rewrite 5.28 becomes;

$$\left(\psi_{\rho\rho} - \epsilon\psi_\rho + \epsilon^2\psi_{\theta\theta} \right) + \beta^2\psi = 0 \tag{5.29a}$$

$$-\psi_\rho = \frac{\mathrm{i}\Gamma^2}{Z}\psi \tag{5.29b}$$

After, the substitution, 4.26, becomes;

$$\beta^2 = \Gamma^2 - \frac{(1-\Gamma)^2}{M^2} \tag{5.30}$$

Now using the formal asymptotic expansion for ψ, β, and Γ, we have;

$$\psi = \psi_0 + \epsilon\psi_1 + \mathcal{O}(\epsilon^2), \ \Gamma = \Gamma_0 + \epsilon\Gamma_1 + \mathcal{O}(\epsilon^2), \ \beta = \beta_0 + \epsilon\beta_1 + \mathcal{O}(\epsilon^2) \tag{5.31}$$

Substituting 5.31, in 5.29, and 5.30, and collecting the $\mathcal{O}(1)$, terms, yields;

$$\psi_{0,\rho\rho} + \beta_0^2\psi = 0 \tag{5.32a}$$

$$\psi_\rho = \frac{\mathrm{i}\Gamma_0^2}{Z}\psi \tag{5.32b}$$

$$\beta_0^2 = \Gamma_0^2 - \frac{(1-\Gamma_0)^2}{M^2} \tag{5.32c}$$

The solution to 5.32a, is given by $\psi_0 = A e^{\mathrm{i}\beta_0\rho} + B e^{-\mathrm{i}\beta_0\rho}$. But, with a strong hint from the outer solution ψ_{out}, the matching criterion dictates, that $\psi_0 = B e^{-\mathrm{i}\beta_0\rho}$. The boundary condition 5.32b, gives the following relation, $\beta_0 = \frac{\Gamma_0^2}{Z}$, which in turn, along with 5.32c gives a 4th order algebraic equation;

$$\frac{\Gamma_0^4}{Z^2} = \Gamma_0^2 - \frac{(1-\Gamma_0)^2}{M^2} \tag{5.33}$$

The axial wave number is given by;

$$\kappa = \frac{\omega - \Omega}{M} = \frac{\omega}{M}(1-\Gamma) \approx \frac{\omega}{M}(1-\Gamma_0) \tag{5.34}$$

The Lorentz transformed axial wave number σ, approximated to the first order is given by;

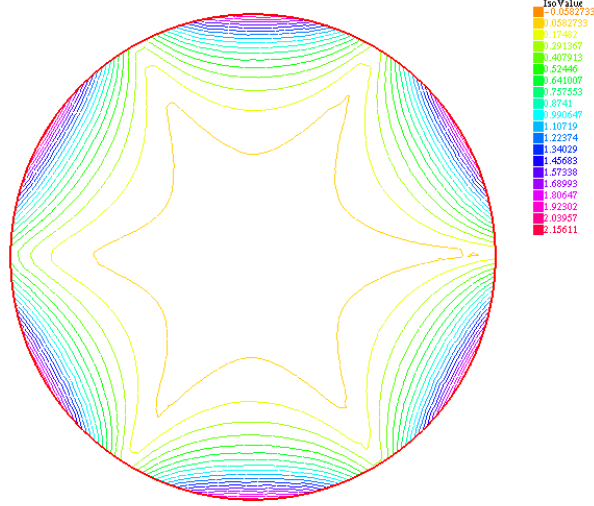$$\sigma \approx \frac{1 - (1-M^2)\Gamma_0}{M} \tag{5.35}$$

37

Figure 5.3: Surface wave profile as given by the eigen function ϕ_{36}, for $M = 0.3$, $Z = 2 - 1$i, and $\omega = 50$

Considering $M = 0.3$, $Z = 2 - 1$i, and $\omega = 50$, it was found that one of the roots of 5.33, is $\Gamma_0 = 0.7752 + 0091$i, which on substituting in 5.35, gives, $\sigma_{\text{analytical}} = 0.98175 - 0.0277$i. The eigenfunction ϕ_{36}, gives a profile of a surface wave, as shown in the figure-5.3, and the corresponding $\Omega = 38.7594 + 0.5057$i. As $\Omega = \Gamma\omega$, this implies $\Gamma_{\text{numerical}} = 0.7751 + 0.0101$i. Therefore, $\sigma_{\text{numerical}} = 0.9819 - 0.0306$i.

The elliptic cross-section

The same form of analysis can be done for an elliptic cross section too, but instead of using the circular polar coordinates one has to use the elliptic coordinates (μ, θ). The Ansatz remains the same, and so does the assumption of solution being periodic in θ. Let a, and b be the major and minor axis of the ellipse respectively, and the focus $c = \sqrt{|a^2 - b^2|}$. 4.25, and 4.26, becomes;

$$\frac{\epsilon^2}{c^2(\sinh^2 \mu + \sin^2 \theta)} \left(\psi_{\mu\mu} + \psi_{\theta\theta} \right) + \beta^2 \psi = 0 \tag{5.36a}$$

$$\frac{1}{c\sqrt{(\sinh^2 \mu + \sin^2 \theta)}} \epsilon \psi_\mu = \frac{\Gamma^2}{\mathrm{i}Z} \psi \tag{5.36b}$$

Again the outer solution, as seen in the circular case, happens to be $\psi_{out} = 0$. The behaviour of the solution in the boundary layer is obtained by scaling $\mu = \mu_0 - \epsilon\rho$, where

38

$\mu_0 = \sinh^{-1}\left(\frac{a}{\sqrt{|a^2-b^2|}}\right)$. With the same approximations as done for the circular case, 5.36, simplifies into;

$$\frac{1}{c^2(\sinh^2\mu_0 + \sin^2\theta)}\left(\psi_{\rho\rho} + \epsilon^2\psi_{\theta\theta}\right) + \beta^2\psi = 0 \tag{5.37a}$$

$$-\frac{1}{c\sqrt{(\sinh^2\mu_0 + \sin^2\theta)}}\psi_\rho = \frac{\Gamma^2}{iZ}\psi \tag{5.37b}$$

With the same expansions given 5.31, and approximating to the the first order we find that, the relation 5.32c, remains the same, and 5.37, becomes;

$$\frac{1}{c^2(\sinh^2\mu_0 + \sin^2\theta)}\psi_{0,\rho\rho} + \beta_0^2\psi_0 = 0 \tag{5.38a}$$

$$\frac{1}{c\sqrt{(\sinh^2\mu_0 + \sin^2\theta)}}\psi_{0,\rho} = \frac{\Gamma_0^2}{iZ}\psi_0 \tag{5.38b}$$

The solution to 5.38a, is $\psi_0 = \mathrm{V}e^{iG\rho} + \mathrm{W}e^{-iG\rho}$, where $G = c\sqrt{(\sinh^2\mu_0 + \sin^2\theta)}\beta_0$. With, the matching criterion, the solution becomes, $\psi_0 = \mathrm{W}e^{-iG\rho}$, and further using the boundary condition, we get the same relation between β_0, and Γ_0, as for the circular case. Thus for leading order approximation, 5.33 remains the same. Using the same values of M, ω, and Z, we found that the eigenfunction ϕ_{71}, gave a profile of surface wave. Thus using the corresponding value of Ω obtained, we were able to calculate the value of σ, which turned out to be, $\sigma_{\text{numerical}} = 0.9833 - 0.0304i$. Comparing it with the $\sigma_{\text{analytical}}$, we can see that, indeed the program is able to locate a surface wave for an elliptical cross-section too as shown by figure-5.4.

The circle-ellipse: Hamster Pouch

Further steps were taken towards arbitrary shaped cross-section, by considering a circle-ellipse combo as shown in figure-5.1d. With the same parameter values in previous cases, the program's output gave a surface wave profile for eigenfunction ϕ_{88}, as shown in figure-5.5. The value of σ, for this particular case turned out to be, $\sigma_{\text{numerical}} = 0.9821 - 0.0296i$. The interesting point to note, is that this matches perfectly with the $\sigma_{\text{analytical}}$.

To conclude this section, table-5.3 is the sum and total of the entire work done here.

5.3.3 Rate of convergence: Newton's method

The Newton's method can go in for further analysis for its convergence. As a first step, we can compare the the iterations with the exact solution, which is available for a circle
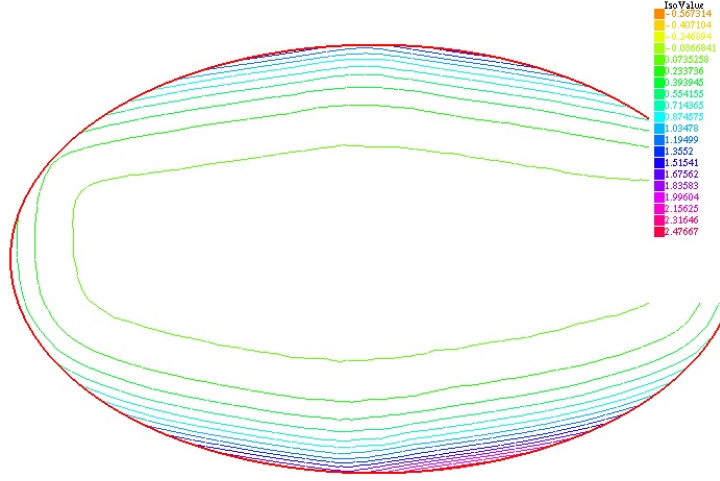
Figure 5.4: Surface wave profile in elliptic cross-section as shown by eigenfunction ϕ_{71}, for $M = 0.3$, $Z = 2 - 1\mathrm{i}$, and $\omega = 50$
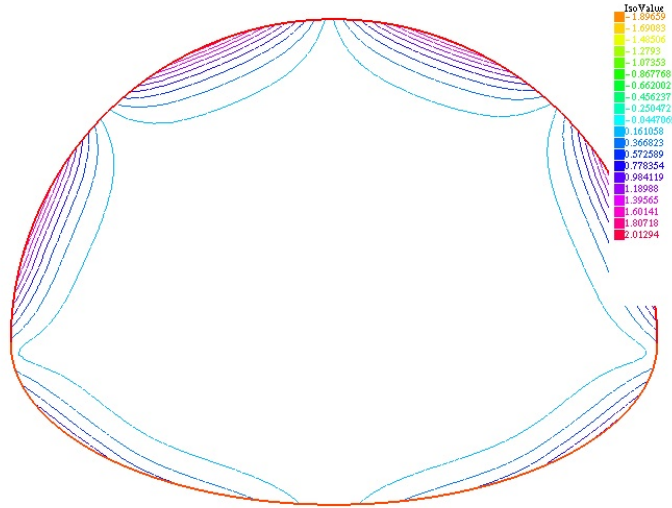

Figure 5.5: Surface Wave profile in circle-ellipse combo as shown by eigenfunction ϕ_{88}, for $M = 0.3$, $Z = 2 - 1\mathrm{i}$, and $\omega = 50$

and then give some preliminary conclusion about its convergence. Taking cue from the analysis previously done, here again we consider a unit circular cross-section, for which

Cases	σ
Asymptotic	$0.98175 - 0.0277\text{i}$
Circle	$0.9819 - 0.0306\text{i}$
Ellipse	$0.9833 - 0.0304\text{i}$
Hamster Pouch	$0.9821 - 0.0296\text{i}$

Table 5.3: Axial wave number:- $Z = 2 - 1\text{i}$, $\omega = 50$, $M = 0.3$

the eigenvalues can be obtained by solving equation-5.22. With exact solution known, one can get an idea of the rate of convergence of the Newton's method. For this convergence purpose, $P2$ basis functions, which refer to the piecewise continuous and quadratic basis functions were used over the approximated finite element space. Since the Newton iteration here implies solving at each stage a finite element eigenvalue problem at each iteration, one might see the cropping up of errors from the finite element method, and the eigen value solver itself. For the present case, three arbitrary modes were chosen, whose corresponding eigenvalues were compared with the analytical solution obtained using 5.22.

Sr.no	Exact solution	1st error	2nd error	3rd error
1.	$10.3245 + 0.5287\text{i}$	0.3708	0.00056	0.00055
2.	$11.9931 + 0.4642\text{i}$	0.5864	0.00911	0.00079
3.	$13.4333 + 0.4402\text{i}$	0.3369	0.0055	0.00085

Table 5.4: Newton's method convergence: $Z = 2 + 1\text{i}$, $\omega = 20$, $M = 0.3$

Table-5.4 gives an account of the error at each Newton iteration step, which gives new insights into the method. It can be seen that, for the initial few iterations, the Newton's method has a quadratic rate of convergence, but soon the finite element error, and possible errors from the eigenvalue solver, etc. sets in, which causes noise in the quadratic convergence of Newton's method. But for all practical purposes, we have got a good estimate of the eigenvalues.

To summarize, in this chapter we started of with different possibilities of solving the non-linear eigenvalue problem. With the platform Freefem++, we were able to find a suitable method of solving eigenvalue problems. Then we designed two methods for iteratively solving the non-linear eigenvalue problem. This was followed up by comprehensive tests for accuracy and convergence with the known analytic solution for a circular geometry. The surface wave profile was used to validate the numerical methods. With a numerical program capable of finding the modes, we move into the next chapter where we construct the profile of modes in the entire duct.

Chapter 6

Simulation of acoustic fields in ducts

In the previous chapter we discussed various numerical methods, for a single cross-section of the duct. Our main goal in this chapter is to extend that scheme for finding the acoustic profile in the entire duct.

6.1 The Variable Ellipse

A slowly varying elliptic lined duct was considered for our study. The elliptic duct was so constructed, such that the cross-sectional area is held constant. Let R_1, and R_2 be the semi-major and semi-minor axes of the ellipse at the opening of the duct. Let R_0, be the radius of the circular end of the duct. In order to maintain constant surface area, we take, $R_0 = \sqrt{R_1 R_2}$ as our circular radius. The duct slowly varies as follows,

$$y = R_0 \left(1 + \sin\left(\frac{\pi X}{10L} \right) \right) \tag{6.1a}$$

$$z = R_0 / \left(1 + \sin\left(\frac{\pi X}{10L} \right) \right) \tag{6.1b}$$

This ensures that the duct has same cross-sectional area throughout. The main reason to have a duct of same cross-section area is to ensure that the mean flow density calculated using 3.14 is constant. This allows us to observe the change in acoustic mode profile purely due to change in the duct geometry. Figure-6.1, gives the profile of the slowly changing elliptic duct under consideration for our study.
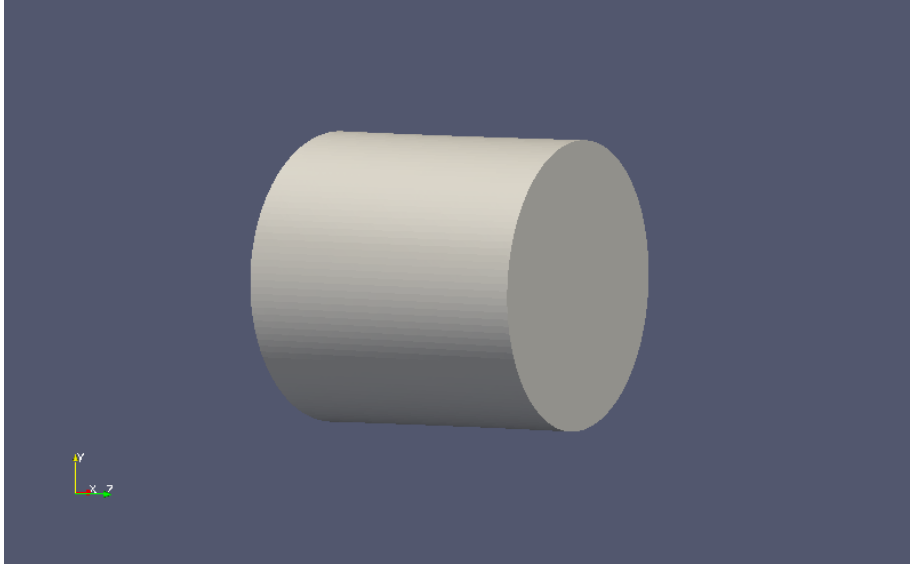
Figure 6.1: Slowly varying elliptic duct with length $L = 2$, $R_1 = 1$, and $R_2 = 0.95$

6.2 Simulation of acoustic profile

With the duct in place, simulations were done for various acoustic modes originating from the fan end, or the circular end of the duct. The mean flow density $D_0 = 1$, and the Mach number $M = 0.3$, at the elliptic opening of the duct. And this remain same throughout the duct, owing to the constant cross-sectional area. The flow in the duct is from left to right, thus the Mach Number M is positive along the length of the duct. Also, the impedance Z, which is a function of the frequency is held constant through the duct. The Freefem++ uses an eigenvalue solver based on Arnoldi's method, and sorts the eigenvalues according to an inbuilt sort algorithm, hence we get an indexed eigenvalues as output. One must be careful with this, as following the same indexing number throughout the duct will result in different eigenvalues at every cross-section. Thus, one needs to use the values obtained from previous cross-section for finding the values of the current cross-section in order to avoid jumps in eigenvalues due to nature of the software.

For starting the iteration process at the circular end of the duct, one of the three starting points as given by 5.3, 5.4, or 5.5. As we are using the Newton iteration, to ensure convergence we take 5.5 for starting point at the circular end. For further cross-sections, for starting point we solve equation of the type 5.8. With the modes assumed to be slowly varying, we can safely assume that the eigenvalues also change slowly. This gives us a way of following the same mode from the starting of the duct till the end. In a circular

cross-section, the solution of the acoustic field can be given by,

$$\psi(r,\theta) = e^{i\omega t - im\theta - i\mu x} \mathcal{J}_m(\alpha r) \tag{6.2}$$

where m can be a positive or negative integer for the same α, due to the symmetry in m. As a result, also linear combinations like

$$\psi(r,\theta) = e^{i\omega t - i\mu x} \cos(m\theta) \mathcal{J}_m(\alpha r) \quad \text{or} \quad e^{i\omega t - i\mu x} \sin(m\theta) \mathcal{J}_m(\alpha r)$$

are equivalent modes. On the other hand, although equivalent, they are physically different. Modes of the form (5.3) rotate in θ as time t goes on, while a mode in the other form remains stationary in circumferential direction. This circular symmetry does not exist with the elliptic duct. So there we can expect only stationary modes, and in the limit of the ellipse approaching a circle, we can only expect the elliptic mode to become a circular mode of stationary type.

Another problem that can occur is "flipping", due to the arbitrariness in sign of an eigenfunction, even when it is normalized. This has been fixed on an ad-hoc basis as follows.

Consider, a, and b as the semi-major and the semi-minor axis respectively, for a given elliptic cross-section. Let ψ, be the eigenfunction on the this cross-section. For the eigenfunctions considered it was seen that the position $[a\cos(\pi/4), b\sin(\pi/4)]$, on the boundary was holding a local extrema for the eigenfunction, which flipped while simulating through the duct. Thus, in order to stop flipping, we define the new eigenfunction as,

$$\psi = \frac{\psi}{\psi(a\cos(\pi/4), b\sin(\pi/4))} \tag{6.3}$$

The above function now can be normalized for obtaining the field, as seen before. This type of treatment is only a temporary fix to the problem, but works well for the cases considered.

With the normalized eigenfunction ψ_n known, we can further find the Amplitude $N(X)$, from equation-4.37. We have taken constant $Q = 1$ in 4.37, for simulation, thus finding the cross-sectional velocity potential Ψ_0, of the first order. The complex acoustic perturbation pressure is given by 4.22, and one can see that for the $\mathcal{O}(1)$ approximation,

$$\hat{p} = -D_0 i\Omega \Psi_0 \exp\left(i\int^x \mu(\epsilon\xi;\epsilon)d\xi\right) \tag{6.4}$$

We can see that $\mathcal{O}(1)$ approximation of acoustic pressure is proportional to the velocity potential $\hat{\phi}$ approximated to the first order. Hence for viewing the acoustic profile, we do the visualization of

$$\text{Re}\left(\Psi_0 \exp\left(i\int^x \mu(\epsilon\xi;\epsilon)d\xi\right)\right)$$

44
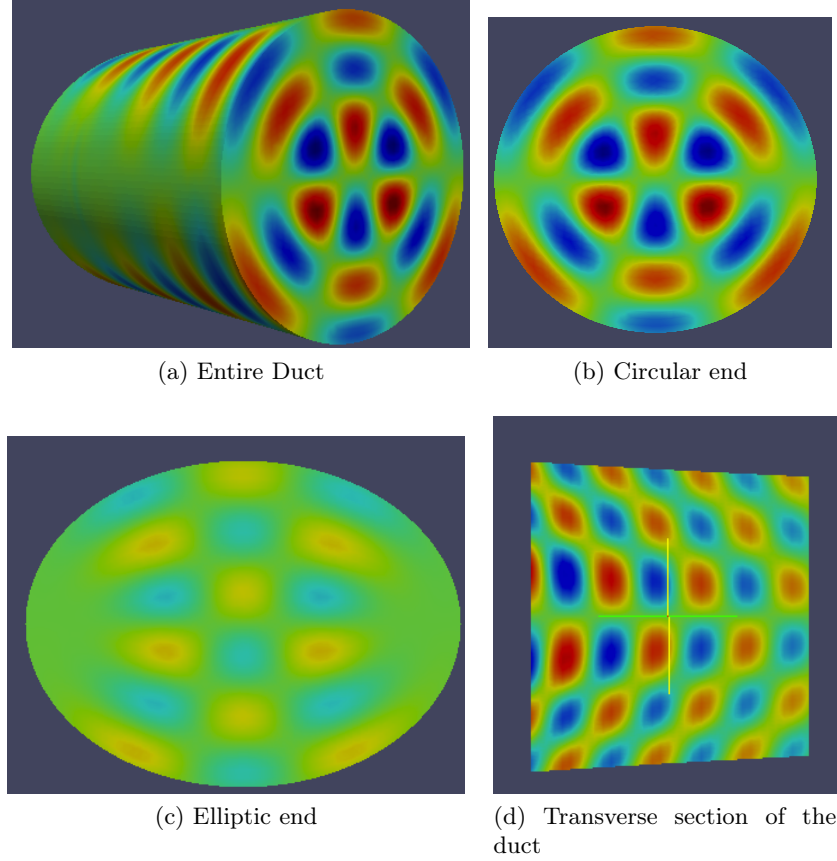
(a) Entire Duct

(b) Circular end

(c) Elliptic end

(d) Transverse section of the duct

Figure 6.2: Pressure distribution of cut-on right running mode for m=3, with $\omega = 20$, $Z = 2 + \mathrm{i}$, $M = 0.3$

With all the problems cleared for time being, we go on to visualize few of the acoustic modes. The software used for visualization is Paraview 3.10.1, which is an open source software developed by Kitware. The .csv files generated by the program were used to supply necessary inputs for visualization. Given the limitations of time and computing, only acoustic modes generated by $P1$ basis functions are visualized. For visualizing the more accurate $P2$ functions modifications needs to be done to the program which is currently out of the scope of the project. For visualization we have only considered the right running modes, which are downstream with respect to the flow.

Figure-6.2 is the snapshot of the pressure distribution, with the azimuthal number $m = 3$. The acoustic mode visualized in figure-6.2 is a right running mode, where one can not only see the attenuation due the duct lining, but also one can observe the way the acoustic mode has changed its profile.
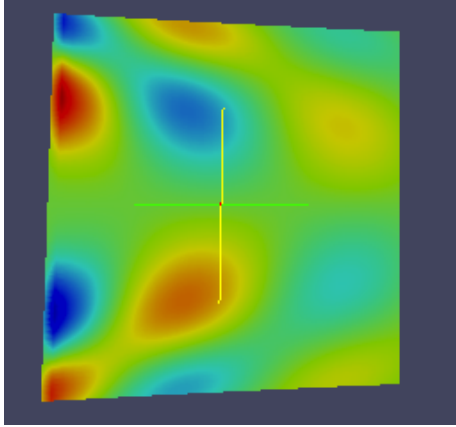
(a) 2nd cut-on mode
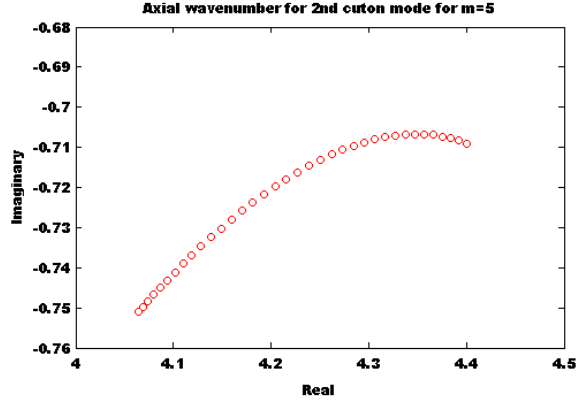
(b) Axial wavenr of 2nd right running (cut-on) mode traced from $x = 0$ ($\mu \approx 4.07 - 0.75$i) to $x = L$ ($\mu \approx 4.4 - 0.71$i)
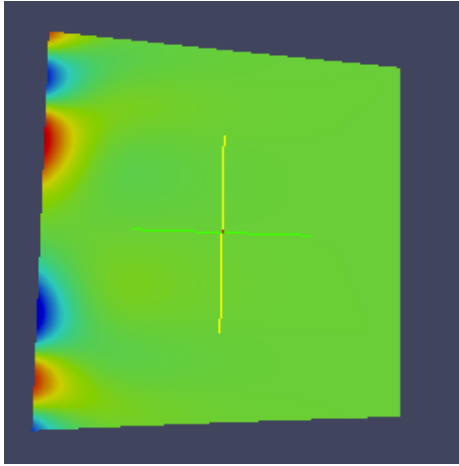
(c) 1st cut-off mode
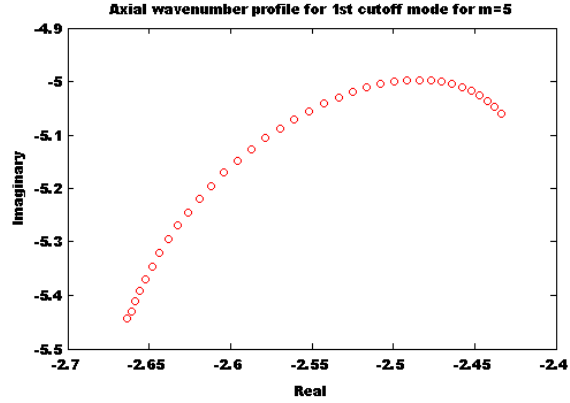
(d) Axial wavenr of 3rd right running (cut-off) mode traced from $x = 0$ ($\mu \approx -2.68 - 5.45$i) to $x = L$ ($\mu \approx -2.43 - 5.05$i)

Figure 6.3: Snapshot of pressure distribution of right running mode with m=5 ($\omega = 13$, $Z = 2 + $i, $M = 0.3$)

In figures-6.3 and 6.4, we analyse the right-running acoustic modes with same azimuthal number m, but with different radial number (as long as we can talk about the radial order by counting the number of extremes in radial direction). The snapshot of the vertical-section of the duct, gives an insight into the propagation of a mode through the duct. In figure-6.3, for the modes with azimuthal number $m = 5$, we find that the mode with radial number $n = 2$ is a cut on mode, whereas the mode with radial number $n = 3$, is a cut-off mode. Similarly in figure-6.4, for the azimuthal number $m = 4$, we see that the first, and

the second modes are cut-on whereas the third mode is a cut-off right running mode. The values of the axial wavenumber corresponding to each mode was traced through the duct, and the results were in perfect accordance to the speculation done earlier about the cut-on and cut-off[1] mode in a lined duct.

Now we concentrate on how the change in frequency affects the modes. In figure-6.5, we see the effect of change of frequency on the nature of an acoustic mode. We find that with the increase in frequency the mode which was cut-off, becomes a cut-on mode. At $\omega = 16$, the mode has just become a cut-on mode suggesting that the change over point must be somewhere close by. If this happened in a hard-walled duct, such a frequency would be called a resonance frequency.

Going further towards the effect of change of Mach number on the nature of acoustic modes. Changing Mach number implies that, changing the mean flow. In the previous paragraphs we have more often been using the word Doppler shift, in union with the mean flow. Now we like to confirm the presence of the same. For doing so, we choose to compare the modes at two different Mach numbers, viz. $M = 0.3$, and $M - 0.01$. It can be seen from figure-6.6, where the modes with azimuthal number $m = 5$, show the effect of mean flow while propagating through the duct. it can be seen that the modes in regime of $M = 0.01$, the axial wavelength is less compared to the wavelength of the modes in the regime of $M = 0.3$. Since the right running modes are propagating downstream with respect to the mean flow, we see that the modes appear to be stretched, thus increasing the axial wavelength.

---

[1]**A note on cut-on and cut-off**. For a hardwalled duct, the modes are either cut-on or cut-off in nature. A cut-on mode propagates forward through the duct, whereas the cut-off mode exponentially decays off. A cut-on mode has the axial wavenumber purely real, and a cut-off has the axial wavenumber, purely imaginary. In case of uniform mean flow, we have to subtract a Doppler shift from the axial wave numbers, but then the notion of cut-on and cut-off is again well defined. However, its definition for a lined duct is a little vague, as the axial wavenumber μ becomes always complex and we can speculate how to characterize the modes in a suitable way in terms of cut-on and cut-off. For a null mean flow case, the mode may be called cut-on if $|\text{Re}(\mu)| > |\text{Im}(\mu)|$, and cut-off if $|\text{Im}(\mu)| > |\text{Re}(\mu)|$. With uniform mean flow, the same speculation holds good if we include the Doppler shift. With non-uniform mean flow there is no single Doppler shift and it becomes unclear how to compare the real and imaginary parts of the modal wave number. In our case, we stick to the above mentioned definition, but with the proviso that sometimes the difference is not clear.
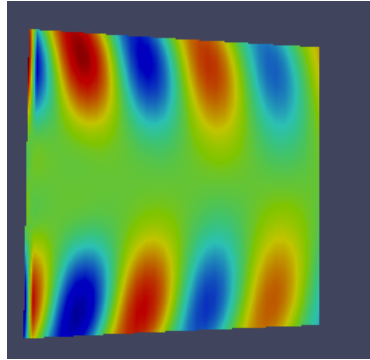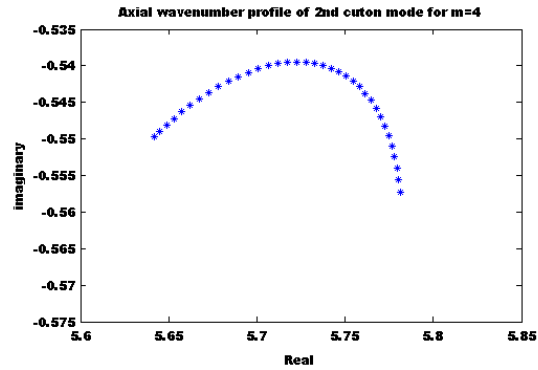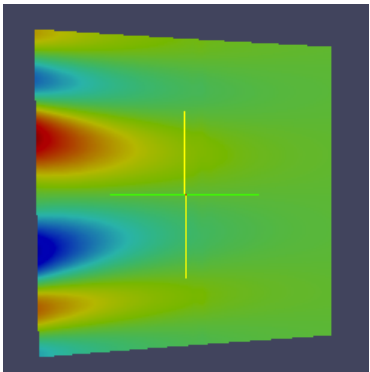
(a) 1st cut-on mode
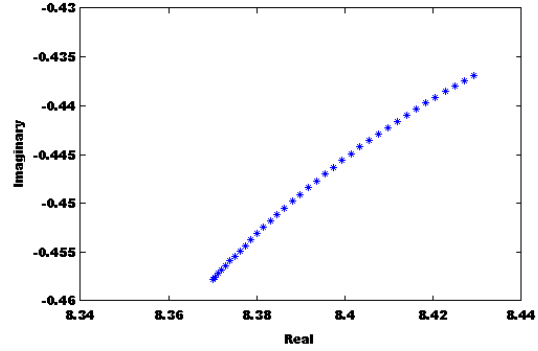
(b) Axial wavenr traced from $x = 0$ ($\mu \approx 8.37 - 0.45i$) to $x = L$ ($\mu \approx 8.43 - 0.43i$) of 1st mode (cut-on)
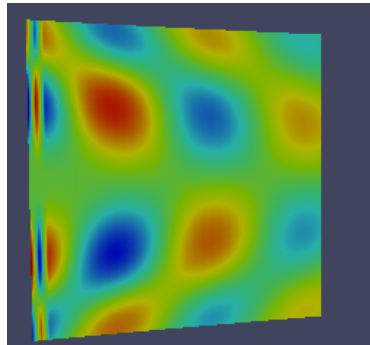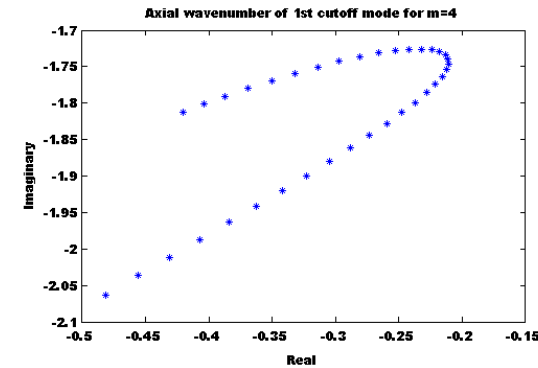

(c) 2nd cut-on mode

(d) Axial wavenr traced from $x = 0$ ($\mu \approx 5.64 - 0.55i$) to $x = L$ ($\mu \approx 5.78 - 0.56i$) of 2nd mode (cut-on)
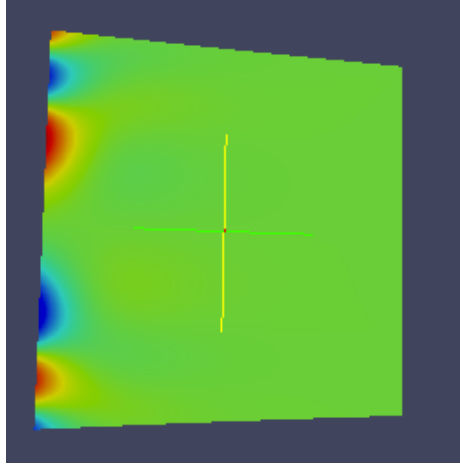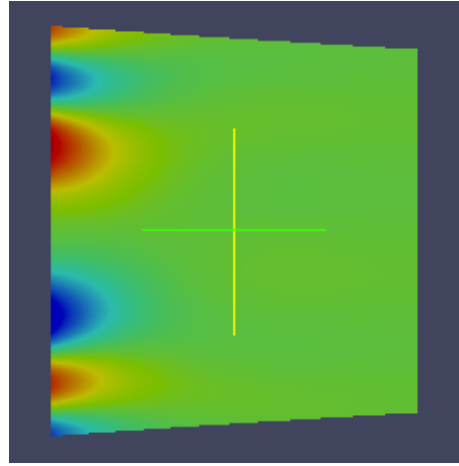

(e) 1st cut-off mode

(f) Axial wavenr traced from $x = 0$ ($\mu \approx -0.46 - 1.8i$) to $x = L$ ($\mu \approx -0.48 - 2.1i$) of 3rd mode (cut-off)
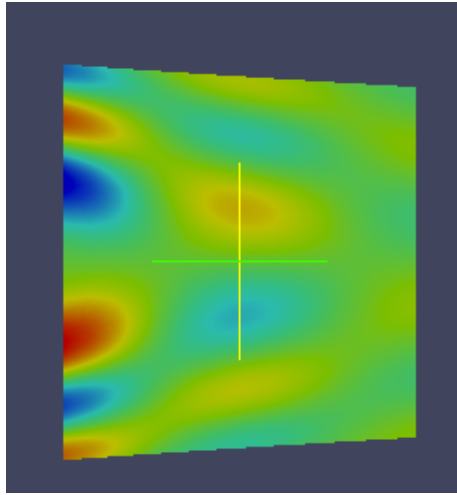
Figure 6.4: Snapshot of pressure distribution of right running mode with m=4 ($\omega = 13$, $Z = 2 + i$, $M = 0.3$)

48

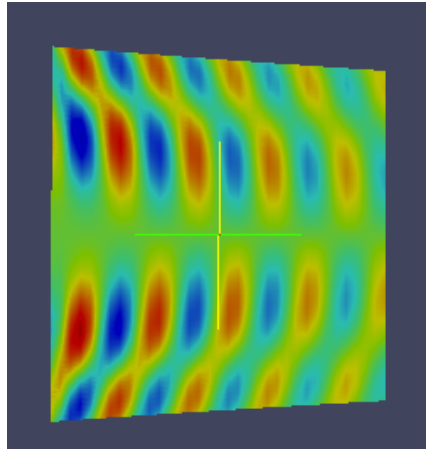(a) 3rd (cut-off) mode for $\omega = 13$
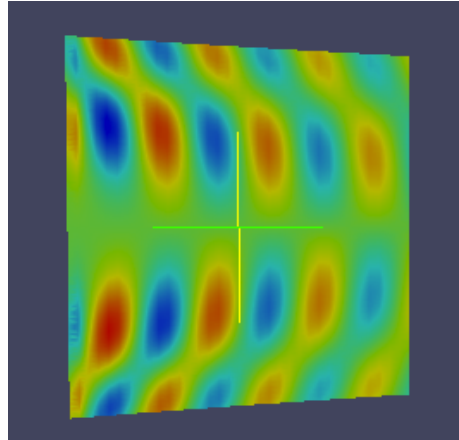

(b) 3st (cut-off) mode for $\omega = 14$
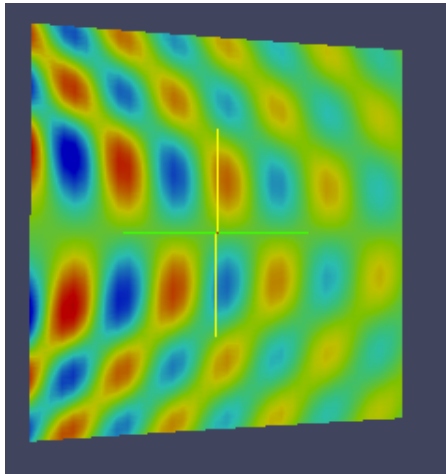

(c) 3rd (cut-on) mode for $\omega = 16$

Figure 6.5: Snapshot of pressure distribution of right running mode with m=5 ($Z = 2 +$ i, $M = 0.3$)
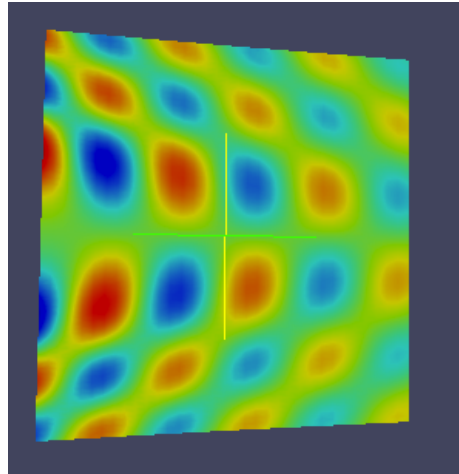
(a) 2nd cut-on mode for $M = 0.01$

(b) 2nd cut-on mode for $M = 0.3$

(c) 3rd cut-on mode for $M = 0.01$

(d) 3rd cut-on mode for $M = 0.3$

Figure 6.6: Snapshot of pressure distribution of right running mode with m=5 ($\omega = 20, \quad Z = 2 + \mathrm{i}$)

Chapter 7

Conclusions and Discussions

As a concluding remark, we like to close this thesis with a summary of the entire work, and also give a glimpse of the road ahead for such topics. The motivation for this work was based on the non-circular, and slowly varying lined intake ducts of jet engines. Rienstra[3] gave a mathematical model for the such ducts with arbitrary cross-sections, where the governing equations of acoustic perturbations were obtained using the WKB method. The resultant equation out this approximation was a non-linear eigenvalue problem based on the Helmholtz equation, thus necessitating use of numerical schemes for solving the same. It was clear that the equation was solvable for cases such as circle, but when the geometry of the duct became arbitrary numerical schemes were pitched in to solve for the same. Thus, the entire problem was based in numerically solving the nonlinear eigenvalue problem. Further the amplitude was obtained using the $\mathcal{O}(\epsilon)$ equation of the asymptotic approximation.

The non-linear eigenvalue problem to be solved is given by 4.25, and 4.26. The coupling of the eigenvalue to the Robin boundary condition is the reason for the system being non-linear. For solving it numerically the Finite Element Method was chosen. Solving involved iterative processes where at each step we solve a standard eigenvalue problem using FEM. The free software Freefem++ was used to the programming. Successive iteration method or simple iteration method, and Newton iteration method were developed to solve the non-linear eigenvalue problem. In either case, the parameter which was iterated upon was Ω, and in case of the Newton's method, the eigenvalues were considered function of Ω, and then the dispersion relation given by 4.26, was used to create a function, whose roots were the desired answer.

With the exact solution known for 4.25, in case of a circular geometry, it was used for verifying the results obtained from the numerical programs. It was seen that the Newton iteration converged really quickly, provided we start near enough to the solution. The effect of using different finite element basis function was also found, and as expected the $P2$ finite

elements gave more accurate results for higher number of eigenvalues compared to its $P1$ counterpart. Then we speculated on the existence of surface waves, which (by definition) are found to exist only near the boundary but decay exponentially inside. By carrying out approximations using matched asymptotic expansions, we were able to compare with the results obtained numerically, which matched the predicted value quite accurately. With the numerical methods firmly in place, we went further to simulate the acoustic profile inside the duct with elliptic cross section. After overcoming the difficulties posed by the software with respect to simulation, we were able to study the acoustic mode patterns inside the duct. The various modes, which are either cut-on or cut-off were visualized using the free software Paraview 3.10.1. The Doppler shift due to change in mean flow was observed, and also the visible effect of a cut-off mode becoming a cut-on mode with change in frequency was observed. The axial wavenumber μ, corresponding to an acoustic mode was traced through the duct, which gave insights on the mode being a cut-on or cut-off.

With the foundation laid, we would like to look into some future scope for this particular project. We like to extend the simulation to cover duct shapes which resemble the actual engine intakes. In our case, we purely concentrated on the downstream acoustic modes, but we would like to see the behaviour of the modes travelling upstream with respect to the mean flow. Another issue which is of great interest in this particular case is that of the rotating mode becoming a non-rotating circumferentially steady mode. At the fan end of the duct we have a circular geometry and the modes emanating from the fan are rotational in nature, which is possible owing to the symmetry of the circle. However, once the circle changed into an ellipse, the modes have no freedom to rotate and we have to focus on a set of stationary modes, equivalent to the rotating mode in the circular duct. At this limiting case, a rotating mode which is given by,

$$\psi(r,\theta) = \mathrm{e}^{\mathrm{i}\omega t - \mathrm{i}m\theta - \mathrm{i}\mu x}\mathcal{J}_{\mathrm{m}}(\alpha r) \tag{7.1}$$

turns into a non-rotating case, by transforming it self into two modes which are circumferentially steady. This transformation needs to be checked for further insights into this behaviour of the acoustic modes.
The Newton's method used for solving the nonlinear eigenvalue problem, has opened up quite a few interesting topics. While using the Newton's method we have assumed continuity of the eigenvalues with respect to the parameter Ω. It was essential to assume it, as we needed to find the derivative for to be used in the Newton's method. Though the continuity was ensured by deliberately avoiding the situations with coalescing eigenvalues, there is no theoretical proof to ascertain the same. Thus, there is an open area to be investigated in terms of the continuity. For simple geometries, it is easy to see the existence of the eigenvalues, but for complicated geometries, we need to find the a way of proving the existence of the eigenvalues. One possible method could be to use the method of continuation in tandem with the Newton's method for solving Robin boundary value problem at each step,

and then try to prove the existence using the convergence of the Newton's method.

Thus, the problem is indeed interesting and challenging both in terms of mathematics and applications. It gives us a method of predicting noise from jet-intakes thus reducing the experimental costs, and time. It also has opened up new mathematical insights due to its nonlinearity with respect to its nonlinearity. The acoustic modes, themselves are mathematically interesting, as they resize and rearrange themselves due to variation in geometry.

Bibliography

[1] J.W.S. Rayleigh. "The Theory of Sound, Volume I and II". Dover edition, New York, 1945.

[2] M.J.T. Smith. "Aircraft Noise". *Cambridge University Press*. Cambridge. 1989.

[3] S.W. Rienstra. "Sound Propagation In Slowly Varying Lined Flow Ducts Of Arbitrary Cross Section". *Journal of Fluid Mechanics*, 495: 157-173. 2003.

[4] S.W. Rienstra and W. Eversman. "A numerical comparison between multiple-scales and finite-element solution for sound propagation in lined flow ducts". *Journal of Fluid Mechanics* , 437: 367 - 384. 2001.

[5] S.W. Rienstra. "Sound transmission in slowly varying circular and annular ducts with flow". *Journal of Fluid Mechanics* ,380: 279 - 296.1999.

[6] N. Peake and A.J. Cooper. "Acoustic propagation in ducts with slowly varying elliptic cross-section" . *J. Sound Vib*, 243: 381- 401, 2001.

[7] S.W. Rienstra. "A classification of duct modes based on surface waves". *Wave Motion*, 37:119 - 135, 2003.

[8] M.K. Myers. "On the acoustic boundary condition in presence of flow". *Journal of Sound and Vibration*, 71:429-434, 1980.

[9] K.U. Ingard. "Influence of fluid motion past a plane boundary on sound reflection, absorption, and transmission". *J. Acoust. Soc. Am.*, 31:1035 - 1036, 1959.

[10] R.M.M. Mattheij, S.W. Rienstra, and J.H.M. ten Thije Boonkkamp. "Partial Differential Equations: Modeling, Analysis, Computation", SIAM, Philadelphia, 2005.

[11] Alan W.Bush. "Perturbation methods for engineers and scientists". CRC press. 1992

[12] A.J. Cooper and N. Peake. " Trapped acoustic modes in aeroengine intakes with swirling flow".*J. Fluid Mech.* , 419:151-175, 2000

[13] W.M.J. Lazeroms. "Sound propagation in slowly varying lined ducts with temperature gradients".Master Thesis, Eindhoven University of Technology, 2010.

[14] S.W. Rienstra and A. Hirschberg. "An introduction to acoustics". Technical Report IWDE 01-03, Eindhoven University of Technology, 2001.

[15] Yousef Saad, "Numerical methods for eigenvalue problems", Manchester University Press, 1992.

[16] G.G. Vilenski and S.W. Rienstra. "On hydrodynamic and acoustic modes in a ducted shear flow with wall lining". *J. Fluid Mech.* , 583:45 - 70, 2007.

[17] George R. C. Tai and Richard Paul Shaw."Helmholtz-equationeigenvalues and eigenmodes for arbitrary domains". *Journal of the Acoustical Society of America*, 56, 1974.

[18] A. Nayfeh, J. Kaiser, and D. Telionis "Acoustics of aircraft engine-duct systems."*American Institute of Aeronautics and Astronautics Journal*, 13:130-153, 1975.